JOURNAL ON

COMMUNICATIONS

VOLUME XLIII. NOVEMBER 1992

OPTICAL COMMUNICATIONS

JOURNAL ON COMMUNICATIONS

A PUBLICATION OF THE SCIENTIFIC SOCIETY FOR TELECOMMUNICATIONS, HUNGARY

Editorial office
Gábor Áron u. 65.
Budapest, P.O.Box 15.
Hungary, H-1525
Phone: (361) 135-1097
(361) 201-7471
Fax: (361) 135-5560

Subscription rates
Hungarian subscribers
1 year, 12 issues 2900 HUF, single copies 360 HUF
Individual members of Sci. Soc. for Telecomm.
1 year, 12 issues 480 HUF, single copies 60 HUF
Foreign subscribers
12 issues 90 USD, 6 English issues 60 USD, single copies 15 USD
Transfer should be made to the Hungarian Foreign Trade Bank, Budapest, H-1821, A/C No. MKKB 203-21411

JOURNAL ON COMMUNICATIONS is published monthly, alternately in English and Hungarian by TYPOTEX Ltd. H-1015 Bp. Batthyány u. 14., phone: (361) 202-1365, fax: (361) 115-4212. Publisher: Zsuzsa Votisky. Type-setting by TYPOTEX Ltd. Printed by HUNGAPRINT, Budapest, Hungary HUISSN 0866-5583

EDITORIAL

The optical transmission and distribution of high speed, high frequency signals is among the fastest growing technologies in telecommunications. On the long term, there is the possibility of monolithic integration of optical and microwave components to produce self-contained devices and subsystems preforming functions in communications, computer networks, process control, test procedures, and other areas. In the near future, hybrid microwave optoelectronic components presumably will lead to new applications such as low cost broad band, distribution networks of high definition television signals (HDTV), high speed chip to chip optical interconnects, microwave-optical links in commercial satellites, high speed subcarrier multiplexed optical local area networks and numerous other applications which cannot be achieved with present technologies. Key, to these developments is the high speed optoelectronics. As a rapidly expanding and maturing area, optoelectronics has many potential applications in the near future.

For enhanced transmission capacities there is an increasing interest in the interfaces of microwaves and lightwaves. This interest has been generated partially by the avaibality of new, high speed, electrooptic devices (diode lasers, modulators, switches, etc.) and partially by the development of more sophisticated microwave and millimeter wave circuits and systems. The present special issue addresses some specific problems of these emerging technologies.

There is a strong trend to apply more and more monolithic microwave-photonic integrated circuits for communications. In the fields of optical transmission and distribution of high speed signals new modulation and detection methods are introduced. The recently developed low noise optical amplifiers extend the application field of the optical transmission of high speed, high frequency signals. These topics are discussed in detail in the present special issue devoted to optical communications.

T. BERCELI

Tibor Berceli received the Dipl.Ing. degree in electrical engineering at the Technical University of Budapest in 1951. From the Hungarian Academy of Sciences, he received the Candidate of Technical Sciences, degree in 1955, and the Doctor of Technical Science degree in 1965. He joined the TKI, Research Institute of Telecommunications, Budapest in 1951. Since that time he investigated surface wave transmission lines, dielectric waveguides, travelling wave amplifiers, reflex klystron oscillators, several kinds of microwave semiconductor oscillators and amplifiers, parametric circuits, up— and dow-converters, injection locked oscillators, etc. His present field of interest is the optical-microwave interaction. Since 1962 he has had a part-time job at the Technical University of Budapest as a Professor of Electrical Engineering. He has taught courses on microwave techniques, active nonlinear microwave circuits, and radio communications systems. Dr. Berceli is the author of 87 papers and six books published in English. He presented 62 papers at international conferences. He was a Visiting Professor at the Polytechnic Institute of Brooklyn in 1964, at the University College London in 1986, at the Drexel University in Philadelphia in 1988-89, and the Technical University of Hamburg-Harburg, Germany in 1991. He was the Chairman of the Organizing Committee for the URSI International Symposium on Electromagnetic Theory in 1986, and the Conference Chairman of the 20th European Microwave Conference in 1990.

MONOLITHIC MICROWAVE-PHOTONIC INTEGRATED CIRCUITS FOR COMMUNICATIONS

P. HERCZFELD

DEPT. OF ELECTRICAL AND COMPUTER ENG.
DREXEL UNIVERSITY
PHILADELPHIA, PENNSYLVANIA, 19104 USA

Some ideas on chip level integration of microwave and photonic components will be presented. The approach is rooted in GaAs MMIC technology, which, however, will require refinement and extension. To confine light into guiding regions will require a more extensive use of heterostructures, resulting in a more complex structure in the vertical direction. With the increasing sophistication of molecular beam epitaxy and related techniques, this should not present a problem. In some cases, feature sizes for the photonic devices in the lateral direction have to be in the order of a half wavelength, or just over .2 microns in GaAs. Fortunately, nanostructure fabrication is a rapidly developing technique, and, in the near future, submicron feature sizes should become more feasible.

1. INTRODUCTION

Two communication technologies will dominate the future developments: satellite and fiberoptic. The new generation of "Advanced Communications Technology Satellites" (ACTs) will provide high quality, high data rate services. In fiberoptic communications we will have megameter transmission systems with no repeaters, better local area networks in offices and factories, and interconnects with high speed computers.

In terms of applications two trends are prevalent. Expansion in global communications through satellite and fiberoptic systems will enhance the integration of third world (and former communist countries) into the western communication manifold. In the western world, emphasis will be on "personal" communications using low orbit satellites and "fiber to the home".

One of the challenges of the future is the development of better interfaces between electronic (microwave) and optical communications, including the chip level merging of photonic and electronic components on III–V compounds.

Maturing of a sophisticated new technology, monolithic microwave integrated circuits (MMIC), marks one of the most important current developments in devices. This new technological base for the design and production of III–V compound-based integrated circuitry is now complete, with sophisticated computer aided design techniques, material and device processing hardware and methodology, testing and packing procedures — all backed by a cadre of expert scientists and engineers.

As a rapidly expanding and maturing area, photonics has many potential applications, both civilian and military. The notion of integrating photonic and microwave devices on a single chip, the theme of this paper, derives from their inherent similarities in terms of material, structure, and fabrication. A key feature of photonic devices and circuits is the invariable interaction between electrons and photons. Therefore, the interface between photonic and high speed electronic processes presents a pivotal scientific and technological challenge, which, in the long term, will lead to new devices and applications. The discussion emphasizes ideas related to chip level integration of microwave and photonic components and subsystems.

2. NOVEL MICROWAVE-PHOTONIC DEVICES

The motivation of the research discussed here is the merging of photonic and microwave componentry on an MMIC substrate, illustrated in Fig. 1. The concept involves addressing MMMICs by optical means to control various microwave functions. Alternatively, the interest lies in retrieving information from MMICs by optical means and routing them via fibers to other microwave circuits. One approach in interfacing MMICs with fiberoptics involves partitioning a section of the standard GaAs chip for the photonic devices, detectors and modulators, while leaving the rest of the MMIC in its normal configuration. This notion supports the constraint that the inclusion of photonic devices on the MMIC chips require minimal changes in standard MMIC design and fabrication practices: a critical point if costs are to be kept in line. The following sections present a discussion of the problem of optical input and output ports on MMICs, augmented by examples.

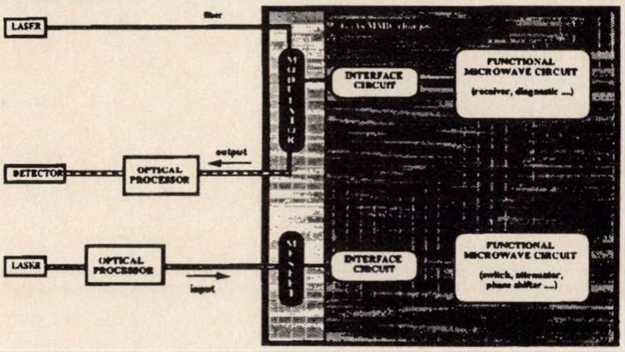

Fig. 1. Control and data signal inputs to MMIC via optical fibers. Standard MESFETs, HEMTs or HBTs are used as optical input ports (detectors). External modulator as an optical output port on MMIC chips.

3. OPTICAL INPUT PORT ON MMIC

The optical control of hybrid and monolithic microwave circuits, such as switches, attenuators, phase shifters and mixers, has been described by several investigators [1]–[5]. Madjar and Paolella [6], [7] studied the internal photovoltaic effect in the MESFET, which gives rise to photoresponse in the device. In the internal photovoltaic effect, illustrated in Fig. 2, the absorbed photons modulate the episubstrate barrier, thereby modulating the channel height. In effect, the light acts as an "optical gate". The simplified form of the photoresponse, the drain current, is

$$I_{ds} = g_m V_{ph} = R_{\text{sub}}(qFA_{\text{eff}} - I_{\text{bar}}) \qquad (1)$$

where g_m is the transconductance of the device and V_{ph} is the optically induced photovoltage, R_{sub} is the substrate resistance, F is the incident photon flux, A_{eff} is the effective area between the gate and drain and the gate and source metalization where the light is absorbed. I_{bar} is the dark current through the barrier.

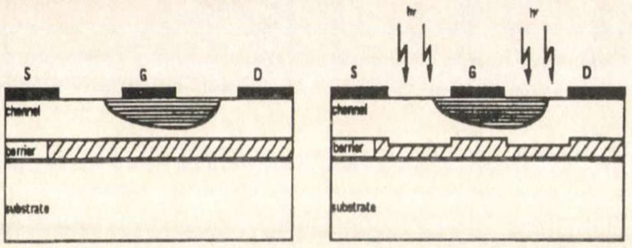

a. b.

Fig. 2. Internal photovoltaic effect in GaAs MESFET. The difference in doping level between the epi and substrate layers produces a potential barrier in the standard MESFET, as shown in Fig. 2a. When illuminated, the potential barrier is reduced, as depicted in Fig. 2b, thereby increasing the channel height (optical gate).

The frequency response of a standard MMIC GaAs MESFETs has been studied analytically and experimentally in the range of 10 MHz to 10 GHz, and compared to a high-speed PIN photodetector [7]. At lower frequencies (below 1000 MHz), the MESFET has a significantly larger response (in excess of 10 dB) than that of the PIN diode, which makes the MESFET desirable as an optical port on MMICs for the detection of low data rate signals. To enhance the high frequency response of the MESFET to the level of the PIN diode, several steps can be taken. The optical coupling efficiency, the fraction of the absorbed to incident photons, is about 60% for the PIN diode, but less then 10% for the MESFET since the metal electrodes block most of the light from entering into the GaAs. By altering the geometry of the device (shorter but larger number of gate fingers), by providing an elliptical spot size (cylindrical lens), and by an antireflection coating on top of the MESFET, the optical coupling efficiency could be enhanced to 40% or higher. This corresponds to a 12 dB increase in the photoresponse resulting in a cross-over point between the MESFET and the PIN responses in the vicinity of 6 to 8 GHz.

Further optimization in the frequency response of the MESFET can be achieved by modifying the doping profile and by increasing the doping ratio between the epi layer and the substrate to reduce the barrier capacitance. This would reduce the RC time constant associated with the internal photovoltaic effect or optical gate and extend the corner frequency. A well designed matching network connecting the MESFET to the microwave circuitry, when implemented in a MMIC configuration, would further reduce cost and improve performance. These measures, when combined with improved coupling efficiency, would result in excellent MMIC optical ports up to 10 GHz.

In a more general sense, a better understanding of photoinduced processes in the MMIC active elements, MESFET, HEMT or HBT, may lead to the design and fabrication of excellent optical ports on MMIC chips.

4. OPTICAL OUTPUT PORTS ON MMICS

The function of an optical output port, as illustrated in Fig. 1, is to bring information out of the MMICs by optical means. The concept introduced here involves sending an optical carrier via a fiber to the GaAs chip where the MMIC generated information is superimposed on the optical carrier. Finally, the coded optical signal is brought out of the chip via the fiber for processing or routing it onward as necessary. This requires the development of an MMIC based external modulator or switch.

Commonly used external modulators are based on the principle of the electrooptic effect to "slow down" the photons. Unfortunately, the electrooptic effect is very small; therefore, either large fields or long interaction lengths, or both, are required to introduce substantial phase modulation. Most devices use an interferometric layout to convert the phase (velocity) modulation into amplitude modulation. The choice of material is $LiNbO_3$, which is not a semiconductor and therefore not suitable for chip level integration with electronics.

An alternate avenue for the index modulation is the use of carrier injection or depletion (i.e., the photo-refractive effect). The dielectric constant, and hence the index of refraction, is a function of the plasma frequency, ω_p, or the carrier density, N, that can be changed by injection or depletion of electrons or holes. For GaAs, at an optical wavelength of 1.3 μm, the change in index of refraction is

$$n - n_0 = \Delta n = (.5n_0) \cdot (\omega_p/\omega)^2 \approx -2.5 \cdot 10^{-21} \text{cm}^{-3} \Delta N_e \qquad (2)$$

where ΔN_e represents the injected carriers. The maximum voltage required to deplete carriers at a Schottky junction is

$$V_{\max} = \frac{eN_D}{2\varepsilon} \cdot d^2 \qquad (3)$$

where d is the Schottky and ohmic contact electrode separation and N_D is the doping density. Carrier injection/depletion can yield a larger change in the index of refraction than can the electrooptic effect. R. Soref et al. [8] have already used the carrier induced solid state plasma effect to make photonic devices.

One of the several device configurations now under consideration is shown in Fig. 3. The structure consists of two vertically integrated optical waveguides fabricated on a semi-insulating substrate (SI-InP). The lower waveguide consists of a 0.4 μm-thick core layer of $In_{0.77}Ga_{0.23}As_{0.50}P_{0.50}$ ($n_1 = 3.4261$), which is grown on a 1.0 μm-thick InP ($n_3 = 3.2091$) buffer layer acting as a passive cladding. The upper waveguide consists of a 0.4 μm-tick waveguide core layer of $In_{0.81}Ga_{0.19}As_{0.40}P_{0.60}$ ($n_4 = 3.3766$). The two core layers are separated by "active" and passive clads. The active cladding is a 0.66 μm-thick 10^{18} cm^{-3} n-doped $In_{0.79}Ga_{0.21}As_{0.45}P_{0.55}$ ($n_2 = 3.39$) layer, and the passive cladding is a 0.2 μm-thick InP layer. On top of the upper waveguide is the final InP layer with a thickness of 1.0 μm. A periodic electrode pattern formed on top of the device provides Schottky contacts while the ground electrode at the bottom of the buffer layer is deposited using a via hole.

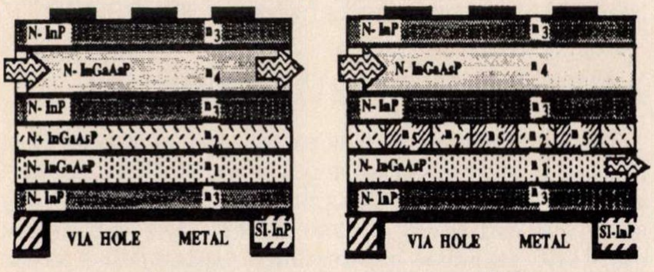

(a) (b)

Fig. 3. Optical switch/modulator structure. With no applied electric field, Fig. 3a, light is guided through the upper waveguide. The electric field depletes carriers under the Schottky contacts forming a grating, through this grating both waveguides are coupled and light is switched from the upper to the lower waveguide.

A preliminary, and greatly simplified, computer simulation of this structure was carried out by M. Silva [9]. The dispersion diagrams for the first two guided modes in the upper and lower guides were simulated with active cladding thickness $a = 0.06\ \mu$m.

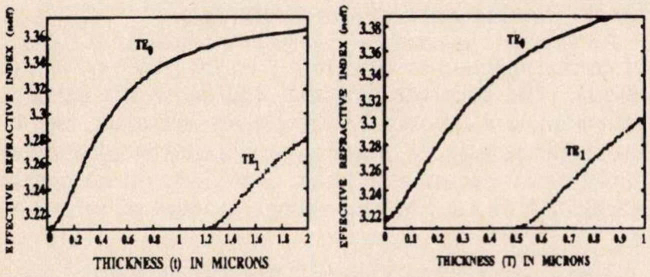

(a) (b)

Fig. 4. Dispersion diagrams of the upper optical waveguide, Fig. 4a, and lower optical waveguide, Fig. 4b, with the above data

The simulation results, shown in Fig. 4, reveal that the upper waveguide is single-mode for $0 \leq t \leq 1.2\ \mu$m while the lower waveguide is single-mode in the range $0 \leq T \leq 0.5\ \mu$m. For a thickness of 0.4 μm the effective refractive index of the upper and lower waveguide is 3.2878 and 3.3326, respectively.

Simulations for the optical intensity and lower waveguide confinement factor were also carried out (Fig. 5).

It can be seen in Fig. 5a that both propagating modes of the structure interact strongly with the electrically generated grating. In Fig. 5b, it can be noted that the lower waveguide confinement factor in the grating region is 7%.

The structure is composed of two nonidentical waveguides and transfer of energy between them occurs via the periodic structure. The period Λ of the grating is chosen to satisfy the phase-matching condition, which is given by:

$$\Lambda = \frac{\lambda_0}{n_{\text{eff}2} - n_{\text{eff}1}} \tag{4}$$

where $n_{\text{eff}2}$ and $n_{\text{eff}1}$ are the effective refractive indices of the lower and upper guide, respectively. At an optical wavelength of 1.3 μm the period of the structure is 29 μm, i.e. 14.5 μm of metal fingers separated by 14.5 μm gaps.

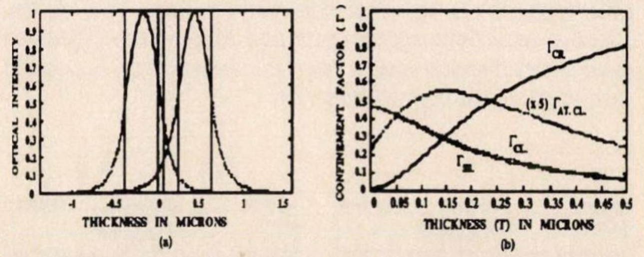

(a) (b)

Fig. 5. Optical intensity versus thickness for both waveguide, Fig. 5a, in this figure the intensity profile at right is for the upper waveguide. The confinement factor versus thickness of the lower waveguide is shown in Fig. 5b.

The voltage required to deplete carriers in the active cladding is approximately 2 volts. Detailed calculations considering the electronics of the complex heterostructure is in progress. Preliminar results indicated that the modulation bandwidth of the device is the GHz range.

This example should be considered as an illustration of the type of novel ideas and devices that may be developed.

5. CONCLUSIONS

Ideas on chip level integration of microwave and photonic components were presented. The approach is rooted in GaAs MMIC technology, which, however, will require refinement and extension. To confine light into guiding regions will require a more extensive use of heterostructures, resulting in a more complex structure in the vertical direction. With the increasing sophistication of molecular beam epitaxy and related techniques, this should not present a problem. In some cases, feature sizes for the photonic devices in the lateral direction have to be in the order of a half wavelength, or just over .2 micron in GaAs. Fortunately, nanostructure fabrication is a rapidly developing technique, and, in the near future, submicron feature sizes should become more feasible [10]. As feature sizes shrink, the transport of free carriers will be dominated by quantum effects, changing the basic interaction between electrons and photons. All these developments represent exciting scientific challenges to be fulfilled by the emergence of novel devices and new applications, ranging well beyond what is envisioned at present.

REFERENCES

[1] Paolella, A. and Herczfeld, P. R., "Optical Gain Control of a GaAs MMIC Distributed Amplifier", *Microwave and Optical Technology Letters*, Vol.1, No.1, March 1988.

[2] Jemison, W., Berceli, T., Paolella, A., Herczfeld, P. R., Kassemset, D., and Jacomb-Hood, A.W., "Optical Control of a Digital Phase Shifter", *1990 IEEE International Microwave Symposium*, Dallas, Texas, May 8 – 10, 1990.

[3] Paolella, A. et al., "Optically Controlled GaAs MMIC Switch Using a GaAs MESFET as an Optical Detector", *1990 MTT-S Symposium Digest*, May, 1990.

[4] Herczfeld, P.R. and Paolella, A., "Optical Gain and Phase Control of a GaAs MMIC Transmit/Receive Module", *Proc. of the 1988 European Microwave Sympmosium*, Sept. 12 – 16, 19088, Stockholm, Sweden.

[5] Bhasin, K. et al, "Control of a GaAs Monolithic Ka-Band Phase Shifter Using a High-speed Optical Interconnect", *IEEE Transactions on Microwave Theory and Techniques*, Vol.38, No.5, May 1990.
[6] Madjar, A. et al., "A Novel Analytical Model for Optically Generated Currents in GaAs MESFETs", Accepted for publication in the *IEEE Transactions on Microwave Theory and Techniques.*
[7] Majdar, A. et al., "Modelling the GaAs MESFETs Response to Modulated Light at RF and Microwave Frequencies", submitted for publication.
[8] Soref, R.A. et al., "Simulation Studies of Silicon Electro-Optic Waveguide Devices", *J. of Appl. Phys.*, November, 1990.
[9] Silva, M., Private communication.
[10] *Proceedings of the IEEE: Special Issue on Nanoelectronics*, August, 1991.

Peter R. Herczfeld received his B.S. degree in Physics from Colorado State University in 1961, his Physics in 1963, and his Ph.D. in Electrical Engineering in 1967, both from the University of Minnesota. Since 1967 he has been on the faculty of Drexel University, where he is a Professor of Electrical and Computer Engineering. He has taught twenty different courses at the graduate and undergraduate level, and lectured extensively in the U.S. and in ten other countries. He is known internationally as an expert in this field, having published over 250 papers in Solid-State Electronics, Microwaves, Photonics, Solar Energy, and Biomedical Engineering. In last three years alone, he has presented at least eight invited papers on the subjects related to this proposal, at IEEE-MTT, IEE-Antennas and Propagation Society, European Microwave Conference, Asia-Pacific Microwave conference, and SMBO conferences. He is the Director of the Center for Microwave–Lightwave Engineering at Drexel, a Center of Excellence which conduct research in microwaves and photonics with over twelve U.S. corporations and government laboratories. He has directed more than fifty-five projects. A memmber of APS, IEEE, SPIE, and the ISEC, he is a recipient of several research and publication awards, including the Microwave Prize. He has served as guest editor for a special issue of the IEEE Transactions on MTT and the Journal of Lightwave Technology on "The Application of Lightwave Technology to Microwave Devices, Circuits and Systems", and now is an associate editor for the Microwave Journal. He is a Fellow of the IEEE.

THE USE OF OPTICAL AMPLIFIERS FOR SIGNAL DISTRIBUTION IN OPTICALLY CONTROLLED PHASED ARRAY ANTENNAS

C. D. ZAGLANIKIS and A. J. SEEDS

DEPT. OF ELECTRONIC AND ELECTRICAL ENGINEERING
UNIVERSITY COLLEGE, LONDON, TORRINGTON PLACE,
LONDON WCIE 7JE, ENGLAND

The paper examines the feasibility of using optical amplifiers in the signal distribution networks of optically controlled phased array antennas. First there is a discussion about which analogue signals need optical amplification in a phased array. Then there is a description of the structure and the principles of operation of the two main types of optical amplifier, the semiconductor laser and the doped fibre structure. Finally, as a specific example, the feasibility of using semiconductor laser amplifiers in the forward link of a satellite-based phased array is analyzed. Using a computer model developed to model analogue optical systems, the optimum position of the amplifiers inside the network in terms of RF link loss, S/N ratio, and total use of semiconductor laser amplifiers can offer reduced electrical power consumption, improved S/N ratio and reduced circuit complexity.

1. INTRODUCTION

Following the successful development of optical amplifiers for the telecommunications industry [1], [2] their use in other applications has been proposed. One of them is in optically controlled microwave phased array antennas for the distribution of the various signals to the elements of the array [3]. One of the main limitations of the passive optical networks currently under research for use in optically controlled phased arrays is the small number of elements (usually about 30) which can be fed from a single optical source. To overcome this problem most designers use many optical sources, each one of them feeding a small number of elements [4], [5], [6]. A microwave network is used to distribute the RF signals to these sources. However, as antenna applications move to higher frequencies the optical sources and other microwave components become more expensive. Also, new, more complicated sources such as laser heterodyne systems are being considered for use in phased arrays [7] with control circuits which are difficult and expensive to construct. So there is a desire to use a single optical source to feed all the elements of the array. This can be done if the output optical signal of this source can be amplified in the optical domain. This can be achieved using optical amplifiers.

Although in the literature the use of optical amplifiers has been extensively examined for digital telecommunications links [1], [8] and cable television distribution systems [9], [10] a recent literature survey has shown that there is no paper which examines the use of laser amplifiers in optically controlled phased array antennas. The object of this paper is to meet that requirement. The paper is organized as follows: first there is a discussion about which signals need optical amplification in a phased array. Then there is a brief description of the structure and principles of operation of the two main types of optical amplifiers, the semiconductor and the erbium doped fibre structure. The characteristics of the two types are discussed with respect to their fabrication methods, polarization and temperature gain sensitivity, optical bandwidth, modulation and noise performance. Finally as a specific example, the feasibility of using semiconductor laser amplifiers in a satellite-based phased array is examined.

2. SIGNALS WHICH MAY REQUIRE OPTICAL AMPLIFICATION IN A TYPICAL PHASED ARRAY

In a typical phased array antenna, both analogue and digital signals need to be distributed from the array processor to the elements and vice versa. The optical technology for the distribution of digital signals is well established and will not be a discussion subject of this paper. The analogue signals which are candidates for the use of optical amplifiers are the following:

2.1. RF and LO signals

These are attractive candidates for optical amplification for two reasons:

- Since these signals need to be distributed to every element of the array, if a passive optical network is used the intensity of the optical carriers will be reduced by splitting and other component losses. So due to the limitations from thermal noise, only a limited number of elements (usually $\simeq$ 30) can be fed from a single optical source. However, if optical amplifiers are used, the splitting losses will be compensated by the gains of the amplifiers and so it may be possible to feed all the elements of the array from a single optical source.
- The frequency of these signals is usually very high. So at these frequencies RF amplifiers and electro-optic converters (laser diodes, electro-optic modulators or heterodyne systems) are difficult and expensive to construct. In contrast the gain of optical amplifiers is not dependent on the modulation frequency. So especially if high RF frequencies are involved it is easier to amplify the signals in the optical than in the electrical domain.

2.2. The return IF signal

In this case it is very unlikely that optical amplifiers will offer any advantage. If a separate optical link with its own dedicated laser and photodiode is used for the transmission of every element signal as suggested in [3], optical amplifiers are not required, since the link distances under consideration are small and there are no losses due to optical splitters or combiners. If the return signals are combined in the optical domain [4], then although there are high excess losses due to the optical combiners these are compensated for by combination gain.

2.3. The IF transmit signal

This signal only exists in certain (usually communication) systems where the mixing is done at the array element level. In such cases as with the RF and LO signals it needs to be distributed to all the elements of the array. So again optical splitting losses will be present, and optical amplifiers will be required if the signal of a single electro-optic source is to be distributed to all the elements of the array. However, since the bandwidth of this signal is usually less than 1 GHz, analysis shows that if semiconductor laser amplifiers are used nonlinearities in the response of the amplifiers may introduce harmonics and third order intermodulation products [11]. To avoid this, the input optical signals to the semiconductor laser amplifiers must be of sufficiently low level that the amplifiers do not operate in their saturation region or the modulation indices of the optical signals must be small. However, if fibre amplifiers are used in the distribution network then the response will be linear for all frequencies of interest.

3. GENERAL CHARACTERISTICS OF OPTICAL AMPLIFIERS

In the literature various types of optical amplifiers have been demonstrated. From these the most important and most widely used are semiconductor laser amplifiers [1], [8] and rare earth doped fibre amplifiers [2]. There follows a discussion af the general characteristics and particularities of these two types of amplifiers with respect to their use in optically controlled phased arrays.

3.1. Structure of semiconductor laser amplifiers

The semiconductor laser amplifier has essentially the same structure as the laser oscillator, but anti-reflection coatings are applied to the laser facets to reduce their reflectivity. In the literature semiconductor laser amplifiers are usually divided into two types: Fabry-Parot (FP) and travelling wave (TW). They differ in their facet reflectivity.

FP amplifiers have high facet reflectivities $(0.01 - 0.3)$ and operate in resonant mode usually just below threshold. Their 3 dB gain bandwidth are small (typical value $\simeq 5$ GHz) [1] so in order to keep the gain constant, the device temperature and current, and the wavelength of the input signal have to be tightly controlled. FP amplifiers also exhibit gain saturation at a lower input power level than TW amplifiers and have lower gain.

TW amplifiers have low facet reflectivities (< 0.01) arising from anti-reflection coatings applied to their facets. TW amplifiers offer wide bandwidth ($\simeq$ 10 THz) while the gain in less affected by temperature. For these reasons only TW amplifiers will be considered for applications in optically controlled phased arrays.

If a laser amplifier has exactly the same structure as a laser oscillator (i.e. the planes of the facets are at $90°$ to the waveguide) then very tight control of the anti-reflection coating process is needed to achieve low reflectivities [12], [13], [14]. A better way to achieve low facet reflectivities is to make the facets of the amplifier at an angle to the waveguide [15], [16], [17]. In this way the light reflected by the cleaved facets does not couple back into the waveguide [15]. This results in an effective facet reflectivity of about 0.02 without anti-reflection coating. The effective facet reflectivity is further reduced to $1.10^{-4} - 8.10^{-4}$ by the application of conventional 0.01 anti-reflection coatings to both facets [16], [17].

Light is usually coupled into and out of the amplifier's waveguide through lens-ended fibres. This requires precise alignment of the fibres and results in optical losses of the order of 3 dB $-$ 5 dB per facet. This considerably reduces the effective gain of the amplifier.

3.2. Structure of fibre amplifiers

Fibre optical amplifiers use optical fibre whose core is doped with a rare earth element, usually erbium or neodymium. Typical doping concentrations vary from a few tenths to a few hundred parts per million [2], [9]. Fibre amplifiers work on the following principle: A pump signal of shorter wavelength than the amplified signal is injected into the fibre. This excites the rare earth ions into a higher energy level thus causing a population inversion. When the signal to be amplified enters the fibre, it stimulates the emission of photons of the same frequency and phase and so is amplified. The pump optical signal can be removed before the receiving photodiode (so that it does not induce extra shot noise) by using an optical filter.

The optimum length of the fibre amplifier depends on the doping concentration, the available pump power, the efficiency, and the gain required [18], [19]. Typical values vary between 1 m and 100 m.

Since fibre amplifiers have essentially the same structure as standard optical fibres, they can be fusion spliced int systems with splicing losses as low as 0.1 dB. This means that unlike semiconductor laser amplifiers they do not have the problem of coupling losses and end-facet reflectivities.

Wavelength of operation of optical amplifiers

The central wavelength of operation of semiconductor laser amplifiers is similar to that of the corresponding laser if its facets were not anti-reflection coated. For fibre amplifiers two wavelengths are of importance:

- The absorption wavelength of the doping ions i.e. the wavelength at which the pump source should be operated
- The fluorescence wavelength of the doping ions which is the wavelength of the input and output signal.

A comprehensive study of the absorption and fluorescence spectra of all except one of the rare earth ions in $SiO_2 - GeO_2 - P_2O_5$ glass has been reported by Ainslie et al [20], and should be consulted for further information.

From all the rare earth elements, erbium and neodymium are the most important since their fluorescence wavelengths are compatible with those used in telecommunications. Erbium ions have absorption wavelengths of interest at 800 nm, 980 nm and 1480 nm. The fluorescence wavelength of interest is 1550 nm which coincides with the third telecommunications window. At this wavelength the bandwidth is about 4 nm ($\simeq$ 500 GHz). The 800 nm absorption wavelength also coincides with that of GaAlAs laser diodes so they can be used as the pump source. Neodymium has absorption bands at 800 nm and 900 nm and fluorescence bands at 1060 nm, 900 nm, and 1320 nm, although high efficiency at this wavelength is hard to obtain.

3.4. Polarization dependence of gain of optical amplifiers

In erbium doped amplifiers, since the structure is cylindrical the gain is the same for both input polarizations. However, in semiconductor laser amplifiers the gain is usually different for the TE and TM polarization modes. This is mainly because the confinment factors Γ are not the same for the two polarization directions. For a typical commercial semiconductor amplifier (BT&D SOA1100/SOA3100) operating at a bias current of 100 mA the gain difference between the two modes is about 4 dB. This difference creates a problem in the use of semiconductor laser amplifiers in optically controlled phased arrays as it introduces an uncertainty in the RF power budget of 8 dB. There are three possible ways to overcome this:

- To calculate for the "worst case" when designing the power budget of the system and then use automatic gain control (AGC) amplifiers in the optical receivers. In this way the final S/N ratio characteristics of the system will be better than the calculated results.
- To construct polarization insensitive semiconductor laser amplifier structures. Various ideas have been reported in the literature [21], [22], [23], [24], [25], [26]. The most important of these are:
  - The design and construction of semiconductor laser amplifier chip structures with equal confinment of the two modes and thus reduced polarization sensitivity [21], [22].
  - The dynamic control of the polarization and temperature characteristics of semiconductor laser amplifiers using an all-electronic method as proposed and demonstrated by Ellis et al [25], [26].

3.5. Temperature dependence of gain of semiconductor laser amplifiers

The gain of semiconductor laser amplifiers also depends on the temperature. For TW amplifiers the main factors which contribute to this are a reduction in the material gain constant B and an increase in the transparency carrier density n_{tr} when the temperature increases. According to [1] for a typical 500 μm length amplifier operating in the wavelength band of 1.5 μm the gain increases with decreasing temperature by about 0.6 dB/°K. As well as the increase in gain when the temperature falls there is also an increase in the passband ripple of the amplifier if there is some residual reflectivity. So for phased arrays which need to operate reliably over a range of temperatures this temperature dependence has to be compensated for.

One way to do this is to use a Peltier cooler and a feedback circuit. Typical commercial amplifiers such as the SOA3100 from BT&D are packaged with a temperature control mechanism containing the Peltier cooler and thermistor. This way of directly controlling the temperature is good for applications in which electrical power is not expensive to supply (for example in ground based phased arrays). However, for space applications where electrical power is expensive this method cannot be used or can be used only if a few amplifiers are present in the array.

An alternative method of controlling the temperature and polarization characteristics of semiconductor laser amplifiers using an all-electronic method has been proposed and demonstrated by Ellis et al [25], [26]. This uses a drop in the bias voltage of the device which depends on the optical signal inside the amplifier to detect the optical power out of the device. Then, by electronically controlling the current to the amplifier, its gain can be kept constant with variations of the temperature and polarization of the input signal.

3.6. Noise characteristics of optical amplifiers

The equations describing the various noise contributions in semiconductor laser amplifiers are presented in Appendix A. These equations have been derived from the mean and variance in the photon number at an optical amplifier output described by the photon master equation [27] and assume a flat frequency response over any reasonable communications bandwidth. Recently a RIN-like behaviour of semiconductor laser amplifiers has been reported [28] but the mechanisms and equations for this have not yet been fully studied in the literature. So in this analysis only the classical noise equations will be used. As can be seen from Appendix A there are four main noise contributions to the total noise of the amplifier; the beat noise between signal and spontaneous emission components, the amplified signal shot noise (quantum noise), the beat noise between spontaneous emission components and the spontaneous emission shot noise.

The noise figure F of an optical amplifier (semiconductor or fibre) is defined as the degradation in the S/N ratio before and after amplification of a quantum noise limited optical signal. If the signal-spontaneous beat noise is predominant over the spontaneous-spontaneous beat noise then using equation (11) of Appendix A the noise figure F can be reduced to the simple expression:

$$F = 2n_{sp}\chi \qquad (1)$$

where n_{sp} is the population inversion parameter and χ the excess noise coefficient for the beat noise between signal and spontaneous emission (for a complete definition of the above parameters see Appendix A). The best theoretical noise figure which can be achieved for an optical amplifier is 3 dB under complete population inversion of the amplifying material i.e. when $n_{sp}\chi = 1$. Erbium doped fibre amplifiers have very low noise figures of the order of 3.2 dB for a co-propagating pump signal and 5.5 dB for a counter-propagating pump signal [29], [30] and in many cases their noise characteristics are nearly quantum noise limited [29]. For semiconductor amplifiers noise figures varying from 5.2 dB for TWA's [31] to 13 dB for FP structures [32] have been reported.

3.7. Electrical power consumption and efficiency of optical amplifiers

Semiconductor laser amplifiers usually have better electrical-optical conversion efficiences than erbium doped structures since the electrical energy is directly converted into optical energy without the intermediate use of a pump signal as in fibre amplifiers. Typical pump power requirements to achieve comparable gains are about 70 mW for a semiconductor laser amplifier and 100 mW of optical power for a rare earth amplifier.In general fibre amplifiers need roughly 5 times more electrical power than semiconductor amplifiers but this depends on many factore such as the efficiency of the pump source and the efficiency of the amplifier. For example several efficient erbium doped structures have been reported in the literature [33], [34]. This low efficiency of fibre amplifiers, unless a very efficient configuration is constructed, makes them unsuitable for use in applications where electrical power is expensive such as satellite-based phased arrays. However, because of their other advantages relative to semiconductor laser amplifiers they should be the choice for ground based and other phased array structures where electrical power is not a significant problem.

4. THEORETICAL ANALYSIS OF THE USE OF SEMICONDUCTOR LASER AMPLIFIERS IN THE FORWARD LINE OF A SATELLITED-BASED PHASED ARRAY

Having discussed the general characteristics of the two types of optical amplifiers, the use of semiconductor laser amplifiers will be analyzed with reference to a specific system. The analysis of a system using fibre amplifiers is similar except that their noise characteristics are usually better. The system under consideration is the forward link of a satellite-based phased array which is currently under development without the use of optical amplifiers [4], [5], [6]. The general characteristics of the link are that it has to distribute a 5.3 GHz chirped transmit signal and a 5 GHz receive local oscillator signal to the 512 T/R elements of the array. The S/N ratio of the output signal should be at least 113 dBc Hz. The input and output signal levels should both be 0 dBm to provide a transparent system.

The current approach uses sixteen 1300 nm high speed lasers each feeding 32 elements. At the remote interface a P-I-N photodiode is used which is reactively matched to a low noise amplifier stage. The signal is then boosted to the required output level using a cascade of six MMIC amplifier chips.

The parameters of the link have been entered into a computer model whose main equations are described in Appendix A, and without the use of optical amplifiers the agreement between the modelled and the experimental results was better than 1 dB. The optical amplifier chosen for the analysis is a polarization insensitive structure constructed by British Telecom Laboratories [21]. It is not yet commercially available though it is expected that it soon will be for both 1500 nm and for 1300 nm. In the analysis the amplifier is assumed to be biased at 115 mA for which current the unsaturated internal gain is about 28 dB. Assuming a typical coupling loss of about 5 dB per facet the unsaturated fibre to fibre gain should be about 18 dB. The calculated results from the program are the following:

Fig. 1. shows the S/N ratio versus total optical attenuation of the link (not including the gain due to the amplifiers) using a) no optical amplifiers b) one optical amplifier and c) two optical amplifiers. In these curves the attenuation between successive optical amplifiers and between optical amplifiers and laser and photodiode was kept the same. It can be seen that using either one or two amplifier stages all the 512 elements of the array can be fed.

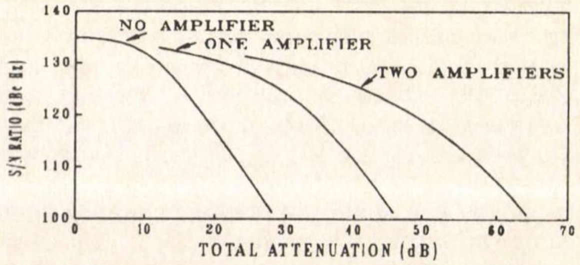

Fig. 1. Modelled S/N ratio versus optical attenuation for the link using a) no semiconductor laser amplifiers b) one semiconductor laser amplifier and c) tow semiconductor laser amplifiers

Fig. 2. shows the RF link loss (from the input of the laser to the load resistance of the photodiode) versus the total optical link attenuation for links containing zero to four optical amplifiers. As in Fig. 1. the attenuation between successive optical components was the same. From the curves it can be seen that for low values of optical attenuation and for more than two amplifiers, net RF link gains can be obtained. Also for low values of attenuation the extra RF gain obtained by placing an additional optical amplifier in the link is reduced as more amplifiers enter the link. This is due to gain saturation of the amplifiers at high input optical powers. However, as the attenuation of the optical link increases the curves diverge from one another increasing the gain contributions from individual amplifier stages.

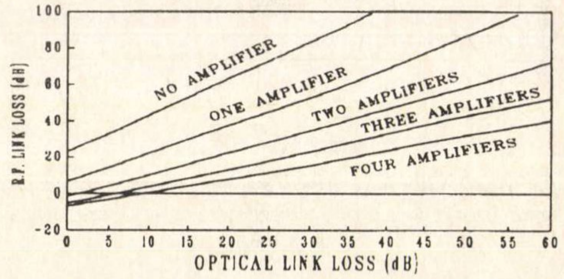

Fig. 2. RF link loss (from the input to the laser to the load resistance of the photodiode) versus optical attenuation for links containing one to four optical amplifiers

Fig. 3. shows the relative contributions of the various noise sources in an optical link containing one laser amplifier. For low values of attenuation, less than 18 dB the laser RIN noise is the dominant source. For medium values of attenuation between 18 and 30 dB the internal amplifier noise dominates. Finally for values of attenuation over 30 dB the link becomes thermal noise limited.

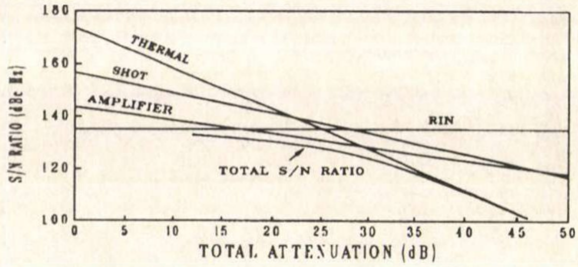

Fig. 3. Modelled S/N ratio of the link using one semiconductor laser amplifier. The various noise contributions can be seen

The internal amplifier noise has its origins in 4 sources [35]. Fig. 4. shows the relative contribution of these sources in the total S/N ration of the link. One of the problems in designing optical networks with laser amplifiers is to determine where to put the amplifiers inside the network in order to achieve the maximum advantage in terms of S/N ratio and RF link loss. For example assume there is an optical link with a certain optical loss and it is required to incorporate an amplifier stage. Where should this amplifier stage be inserted to bring the maximum advantage? The problem has been analyzed using the equations described in Appendix A and Fig. 5. and Fig. 6. show the output S/N ratio and RF link loss as a function of the percentage of the optical attenuation in dB of the link before the optical amplifier. The four curves represent four different total optical link attenuations. It can be seen that the optimum S/N ratio can be obtained if the amplifier is placed somewhere in the middle of the link. This is because when the amplifier is placed near the beginning of the link it operates in its saturation region and so its gain is less than its maximum gain. When it is placed at the end of the link its internal noise contributions become more important as the input optical signal is weaker. The lowest RF link loss can be obtained when the amplifier works in the unsaturated regime. It is thus best placed somewhere between the middle and the end of the link.

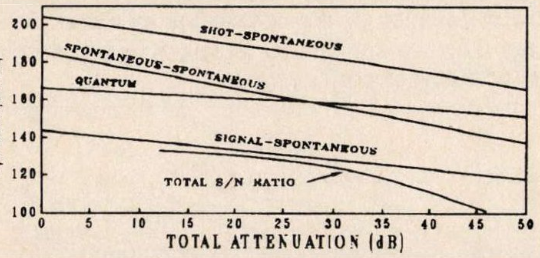

Fig. 4. Modelled S/N ratio of the link using one semiconductor laser amplifier. The various noise contributions due to the laser amplifier can be seen.

When the link has two amplifiers, the problem of where they should be placed inside it to obtain the optimum performance becomes more complex. Fig. 7. and Fig. 8. show the output S/N ratio and RF link loss as a function of the relative positions of the amplifiers inside the link (percentage attenuation in dB before each amplifier).

Fig. 5., 6., 7., 8. are the design curves for point-to-point optical links consisting of one laser and one photodiode. In the case of tree-type distribution networks containing one laser and many photodiodes the total number of amplifiers required for each network implementation has to be taken into account.

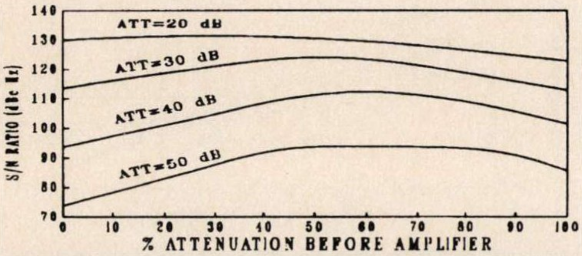

Fig. 5. Output S/N ratio as a function of the position of the amplifier inside the optical link. (% attenuation of the link in dB before the amplifier) for various values of total link attenuation

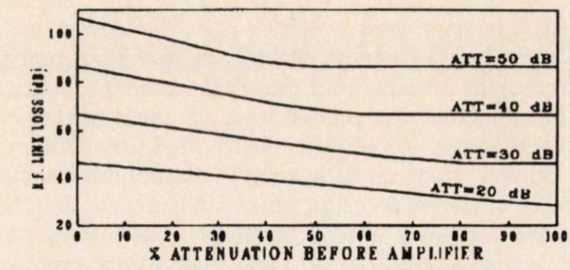

Fig. 6. RF link loss (from the input to the laser to the load resistance of the photodiode) as a function of the position of the amplifier inside the optical link. (% attenuation of the link in dB before the amplifier) for various values of total link attenuation.

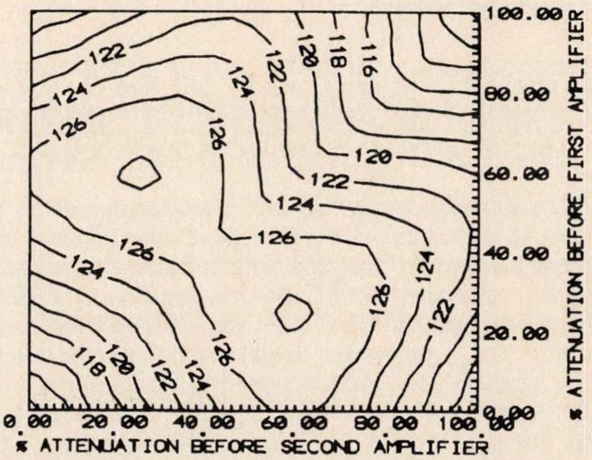

Fig. 7. S/N ratio (constant contours) of a link with 2 amplifiers as a function of the position of the amplifiers inside the link (% passive attenuation in dB before each amplifier). The total optical link loss is 35.6 dB.

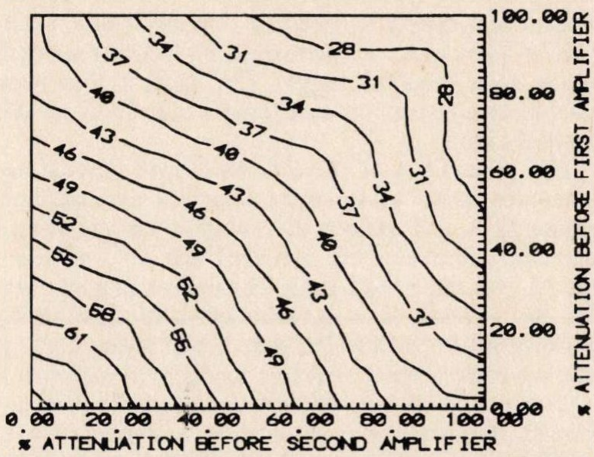

Fig. 8. RF link loss (constant contours) of a link with 2 amplifiers as a function of the position of the amplifiers inside the link (% passive attenuation in dB before each amplifier). The total optical link loss is 35.6 dB.

Based on the above design curves and the technical specifications of the satellite-based phased array proposed by [4], three possible network structures have been designed and analyzed which use semiconductor laser amplifiers. In summary Table 1. shows the main characteristics of the 3 proposed structures. It can be seen that networks 2 and 3 which use optical amplifiers offer superior performance in terms of power consumption and S/N ratio.

Table 1. The main features of the 3 proposed networks

Network No.	No of lasers used	No of optical amplifiers used	Amplification needed after the photodiode to obtain an output power level of 0 dBm. (dB)	Total power consumption (W)	S/N ratio (dBc Hz)
Passive	16	0	55.1	1508	115
1	1	16	52.3	1496	117
2	1	48	31.2	827	125
3	1	272	21.7	617	124

5. CONCLUSIONS

The analysis in this paper shows that optical amplifiers have the potential to offer significant advantages if they are used to amplify the signals in the forward links of optically controlled phased array antennas. The advantages are in terms of power consumption and noise performance. Semiconductor amplifiers usually offer lower power consumption and can be made to operate at all the wavelengths of interest; but they present problems such as polarization sensitivity, complexity of construction etc. However most of these problems are expected to be solved in the near future with the construction of better amplifier structures currently under development in many laboratories. Fibre amplifiers offer simplicity of construction and superior performance characteristics but they need an optical pump source which makes them usually less efficient in terms of electrical power consumption. also performance in the 1300 nm band is limited. So for satellite based phased arrays semiconductor laser amplifiers should be the choice, while for ground based and other structures where electrical power is not very expensive, fibre amplifiers are likely to present the optimum solution.

APPENDIX

Equations to calculate the signal and noise levels in optical links with laser amplifiers are given in the followings.

A. 1. Equations used to calculate the transfer characteristics of a directly modulated semiconductor laser

The unmodulated optical power out of a laser diode is given by:

$$P_{\text{opDC}} = a(I - I_{\text{the}}) \tag{2}$$

where a is the electro-optical conversion efficiency of the laser, I_{the} is the threshold current of the laser and I is the current to the laser. If the laser is resistively matched to the transmission line of the input RF signal the rms value of the modulated optical power out of a laser P_{opRF} is:

$$\mathrm{P_{opRF}} = \mathrm{a}\left[\sqrt{\frac{\mathrm{P_{RF}}}{(\mathrm{R_A}+\mathrm{R_B})}}\right] \tag{3}$$

where P_{RF} is the RF power applied to the laser, R_B is the input impedance of the laser and R_A is the matching resistance.

The noise power modulated onto the optical signal arises from two main factors:

- Noise carried by the electrical RF signal which is modulated on the optical carrier together with the signal. This can be entered into the model using equation (3):

$$\mathrm{P_{opa}} = \mathrm{a}\left[\sqrt{\frac{\mathrm{P_{nse}}}{(\mathrm{R_A}+\mathrm{R_B})}}\right] \tag{4}$$

where P_{nse} is the RF noise power per unit bandwidth carried by the RF signal
- Noise produced by the laser. This is given by:

$$\mathrm{P_{RIN}} = \sqrt{\mathrm{RIN\ P^2_{opDC}}} \tag{5}$$

where RIN is the relative intensity noise of the laser. The total noise modulated on the optical carrier is:

$$\mathrm{P_{opnse}} = \sqrt{\mathrm{P^2_{opa}} + \mathrm{P^2_{RIN}}} \tag{6}$$

A. 2. Equations used to calculate the transfer characteristics of a semiconductor laser amplifier

The equations used to model a semiconductor laser amplifier are mainly a modification of the equations presented in [35]. The unmodulated optical power out of the amplifier is given by:

$$P_{\text{opDC(out)}} = GP_{\text{opDC(in)}} + hf(G-1)n_{\text{sp}}m_t\triangle f_1 \tag{7}$$

where $P_{\text{opDC(in)}}$ is the unmodulated input optical power to the amplifier, G is the gain of the amplifier (from the input to the output facet of the chip) hf is the energy of the input optical signal, m_t is the effective number of modes, n_{sp} is the population inversion parameter and $\triangle f_1$ the equivalent noise bandwidth for the spontaneous emission shot noise. In this equation the first term represents the amplified optical signal power and the second the optical power due to spontaneous emission. The population inversion parameter n_{sp} is given by:

$$n_{\text{sp}} = \frac{n}{n - n_{\text{tr}}} \tag{8}$$

where n is the carrier density inside the amplifier and n_{tr} the transparency carrier density of the amplifier.

It can be proved that the relation between the average carrier density and the single pass gain of the amplifier G_s is:

$$n = \frac{\frac{1n(G_S)}{L} + \alpha_{\text{sc}} + n_{\text{tr}}}{\Gamma B} \tag{9}$$

where α_{sc} is the loss coefficient of the guided mode, Γ is the confinment factor and B is the gain constant of the amplifier.

The equivalent noise bandwidth $\triangle f_1$ for the spontaneous emission shot noise is given by [35], [36]:

$$\triangle f_1 = \sum_{m_t} \frac{(1 + R_1G_s)(1 - R_2)(G_s - 1)c}{(1 - R_1R_2G_s^2)2Ln_e(G-1)} \tag{10}$$

where R_1 and R_2 are the mirror reflectivities of the amplifier, L is the length of the amplifier, c is the speed of light and n_e is the effective refractive index of the amplifier. The summation in the above equation is done over the modes of the amplifier.

The noise power per unit bandwidth modulated on the optical signal at the output of the amplifier has its main origins in two factors:

- Noise modulated on the input optical signal to the amplifier with optical power per unit bandwidth $P_{\text{opnse(in)}}$.
- Noise produced by the amplifier itself. This has optical power per unit bandwidth of:

$$P_{\text{opamp}} = hf\left[\frac{GP_{\text{opDC(in)}}}{hf} + (G-1)n_{\text{sp}}m_t\triangle f_1 + \frac{2G(G-1)n_{\text{sp}}\chi P_{\text{opDC(in)}}}{hf} + (G-1)^2 n_{\text{sp}}^2 m_t \triangle f_2\right]^{\frac{1}{2}} \quad (11)$$

where $\triangle f_2$ is the equivalent noise bandwidth for the beat noise between spontaneous emission components and χ is the excess noise coefficient for the beat noise between signal and spontaneous emission. The four terms on the right hand side of the equation represent amplified signal shot noise (quantum noise), spontaneous emission shot noise, beat noise between signal and spontaneous emission and beat noise between spontaneous emission components.

The equivalent noise bandwidth $\triangle f_2$ for the beat noise between spontaneous emission components is given by [35], [36]:

$$\triangle \mathrm{f}_2 = \sum_{\mathrm{m_t}} \frac{(1+\mathrm{R_1G_s})^2(1-\mathrm{R_2})^2(\mathrm{G_s}-1)^2\mathrm{c}}{(1-\mathrm{R_1R_2G_s^2})^3 2\mathrm{Ln_e}(\mathrm{G}-1)^2} \quad (12)$$

The excess noise coefficient χ for the beat noise between signal and spontaneous emission is given by [35], [36]:

$$\chi = \frac{(1+\mathrm{R_1G_s})(1-\mathrm{R_2})(\mathrm{G_s}-1)}{(\mathrm{G}-1)(1-\sqrt{\mathrm{R_1R_2}}\mathrm{G_s})^2} \quad (13)$$

Finally to calculate the total noise out of the amplifier $P_{\text{opnse(out)}}$ the noise into the amplifier times the gain is added to the noise produced by the amplifier:

$$\mathrm{P_{opnse(out)}} = \sqrt{(\mathrm{GP_{opnse(in)}})^2 + \mathrm{P_{opamp}^2}} \quad (14)$$

In the computer model the gain G versus input optical power curve of the amplifier is entered as a series of data points. Then the computer calculates the gain of the amplifier at every input optical power by drawing straight lines between the points. To calculate the single pass gain of the amplifier equation (4) of Nukai [35] is modified to give:

$$G_s = \frac{1}{\sqrt{R_1R_2}} + \frac{(1-R_1)(1-R_2)}{GR_1R_2} - \left(\sqrt{\left[\frac{1}{\sqrt{R_1R_2}} + \frac{(1-R_1)(1-R_2)}{GR_1R_2}\right]^2 - \frac{1}{R_1R_2}}\right)^{\frac{1}{2}} \quad (15)$$

A. 3. Equations used to calculate the transfer characteristics of a photodiode

The DC current out of a photodiode is given by:

$$I_{\text{dc}} = \frac{\eta P_{\text{opDC}}e}{hf} \quad (16)$$

where P_{opDC} is the unmodulated optical power of the incident signal, η is the quantum efficiency, e is the electronic charge and hf is the energy of an incident photon to the photodiode.

The RF electrical power out of the photodiode P_{RF} is given by:

$$P_{\text{RF}} = \left[\frac{\eta P_{\text{opRF}}e}{hf}\right]^2 R_L \quad (17)$$

Where P_{opRF} is the input modulated optical power to the photodiode. To calculate the noise out of the photodiode, three sources of noise have to be taken into account:

- The noise which is modulated on the optical carrier. This may have as origin the RIN of the laser, noise from the electrical source which modulated the laser etc. The output electrical noise power of the photodiode due to this effect per unit bandwidth is:

$$P_o = \left[\frac{\eta P_{\text{opnse}}e}{hf}\right]^2 R_L \quad (18)$$

where P_{opnse} is the optical power per unit bandwidth of the noise modulated on the input optical signal to the photodiode.

- The shot noise of the photodiode which has power per unit bandwidth:

$$P_{\text{shot}} = 2eI_{\text{dc}}R_L \quad (19)$$

- The thermal noise which is present in all electrical systems and has power per unit bandwidth:

$$P_{\text{thermal}} = kT \quad (20)$$

Where k is Boltman's constant and T is the absolute temperature.

The total noise power P_{nse} out of the photodiode is:

$$P_{\text{nse}} = P_o + P_{\text{shot}} + P_{\text{thermal}} \quad (21)$$

REFERENCES

[1] O'Mahony, M. J., "Semiconductor laser amplifiers for use in future fiber systems", *Journal of Lightwave Technology.*, vol.6(4) pp.531-543, Apr. 1988.

[2] Urquhart, P., "Review of rare earth doped fibre lasers and amplifiers", *IEE Proceedings J.*, vol.135(6), pp.385-407 Dec. 1988.

[3] Wallington, J. R. and Griffin, J. M., "Optical techniques for signal distribution in phased arrays", *G.E.C. journal of research*, vol.2, pp.66-74, 1984.

[4] Williams, N. O., Nawas, M. and Pescod, C. R., "Optical signal distribution for a satellite phased array", *IEE colloq.* digest on optical satellitte links and on-board techniques, digest No.8, London 12. Jan. 1990, pp.16/1-16/6.

[5] Nawas, M., Pescod, C. R., and Williams, M. O., "Technical note TN5200, Preliminary report on the signal distribution and interface system (SDIS) demonstrator design", *technology definition of an advanced SAR study*, GEC Marconi Research Centre, Y/256/103, November 1988.

[6] Nawas, M., Pescod, C. R., and Williams, M. O., "Technical note TN5400, Signal distribution and interface system demonstrator manufacture." *technology definition of an advanced SAR study*, GEC Marconi Research Centre, Y/256/170, December 1988.

[7] Gliese, U., Christiensen, E. L., and Stubkjaer, K. E., "Laser linewidth requirements and imporvements for coherent optical beamforming networks in satellites", *Journal of Lightwave Technology*, vol.9(6), pp. 779-790, June 1991.

[8] Saitch, T., and Mukai, T., "Recent progress in semiconductor laser amplifiers", *Journal of Lightwave Technology*, vol.6(11), pp.1656-1664, Nov. 1988.

[9] Yoneda, E., Kikushima, K., Tsuchiya, T., and Suto, K. I., "Erbium doped fiber amplifier for video distribution networks", *IEEE Journal on Selected Areas in Communication*, vol.8, No.7, pp.1249-1255, Sep. 1990.
[10] Way, W. I., Zah, C. E., Lee, T. P., and Cheung, N. K., "Applications of travelling wave laser amplifiers in subcarrier multiplexed lightwave systems." *Published in ICC'89* (IEEE International Communications Conference) Technical Digest.
[11] Zaglanikis, C. D., and Seeds, A. J., "Computer model for semiconductor laser amplifiers with RF intensity modulated inputs", To be published in *IEE Proceedings Part J* (Optoelectronics) June 1992.
[12] Saito, T., Mukai, T., and Mikami, O., "Theoretical analysis and fabriacation of antireflection coatings on laser-diode facets", *Journal of Lightwave Technology*, vol.LT-3, No.2, pp.288-293, 1985.
[13] Eisenstein, G., and Stulz, S. W., "High quality antireflection coatings on laser facets by sputtered silicon nitride", *Applied Optics*, vol.23(1) pp.161-164, 1984.
[14] Serenyi, M., and Habermeier, H. U., "Directly controlled deposition of antireflection coatings for semiconductor lasers", *Applied Optics*, vol.26, pp.845-849, 1987.
[15] Zah, C. E., Osinski, J. S., Caneau, C., Menocal, S. G., Reith, L. A., Salzman, J., Shokochi, F. K., and Lee, T. P., "Fabrication and performance of 1.5 μm GaInAsP travelling-wave laser amplifiers with angled facets", *Electronics Letters*, vol.23(19), pp.990-992, Sep. 1987.
[16] Zah, C. E., Caneu, C., Shokochi, F. K., Menocal, S. G., Favire, F., Reith, L. A., and Lee, T. P., "1.3 μm GaInAsP near-travelling-wave laser amplifiers made by combination of angled facets and antireflection coatings", *Electronics Letters*, vol.24(20), pp.1275-1276, Sep. 1987.
[17] Zah, C. E., Bhat, R., Menocal, S. G., Andreakis, N., Favire F., Caneau, C., Koza, M. A., and Lee T. P., "1.5 μm GaInAsP angled-facet flared-waveguide travelling wave alser amplifiers", *IEEE Photonics technology letters*, vol.2, No.1, pp.46-47, Jan. 1990.
[18] Shimizu, M., Yamada, M., Horiguchi, M., and Sugita E., "Concentration effect on optical amplification characteristics of Er-doped silica single-mode fibers", *IEEE Photonics technology letters*, vol.2, No.1, pp.43-45, Jan. 1990.
[19] Pederson, B., Dybdal, K., Hansen, C. D., Bjarkelev, A., Povlsen, J. H., Vendeltorp-Pommer, H., and Larsen, C. C., "Deatiled theoretical and experimental investigation of high-gain erbium-doped fiber amplifier", *IEEE Photonics technology letters*, vol.2, No.6, pp.863-865, Dec. 1990.
[20] Ainalis, D. J., Craig, S. P., and Davey, S. T., "The absorption and fluorescence spectra of rare earth ions in silica-based monomode fibre", *IEEE Journal of Lightwave Technology*, No.6, pp.287-293, 1988.
[21] Cole, S., Cooper, D. M., Devlin, W. J., Ellis, A. D., Elton, D. J., Isaac, J. J., Sherlock, G., Spurdens, P. C., and Stallard, W. A., "Polarization-insensitive, near-travelling-wave semiconductor laser amplifiers at 1.5 μm", *Electronics Letters*, vol.25(5), pp.314-315, March. 1989.
[22] Toyonaka, T., Tsuji, S., Haneda, M., and Ono, Y., "Polarization-independent semiconductor optical amplifier module using twin grid rod lenses", *Electronics Letters*, vol.27(11), pp.941-942, May 1991.
[23] Koga, M., and Matsumoto T., "Polarization insensitive optical amplifier consisting of two semiconductor laser amplifiers and a polarization insensitive isolator in series", *IEEE Photonics technology letters*, vol.1, No.12, pp.431-433, Dec. 1989.
[24] Grobkopf, G., Ludwig, R., Waarts, R. G., and Weber, H. G., "Optical amplifier configurations with low poarization sensitivity ", *Electronics Letters*, vol.23(25), pp.1387-1388, Dec. 1987.
[25] Ellis, A. D., Malyon, D. J., and Stallard, W. A., "Control and supervisory of semiconductor optical amplifiers for use in submarine systems", *IEEE Colloquium* Digest No. 1989/119 on "Optical amplifiers for communications", pp.10/1-10/4, Oct. 1989.
[26] Ellis, A. D., Malyon, D. J., and Stallard, W. A., "A novel all electrical scheme for laser amplifier gain control", Proc ECOC 88, Brighton, U.K., pp.487-490.
[27] Shimoda, K., Takashaashi, H., and Townes, C. H., "Fluctuations in amplification of quanta with application to maser amplifiers", *J. Phys. Soc. Japan*, vol.12, pp.686-700, 1957.
[28] Rideout, W., Eichen, E., Schalafer, J., Lacourse, J., and MeLand, E., "Relative intensity noise in semiconductor optical amplifiers," *IEEE Photonics Technology Letters*, vol.1, No.12, pp.438-440, Dec. 1989.
[29] Olshanski, R., "Noise figure for erbium-doped optical fibre amplifiers", *Electronics Letters*, vol.24(22), pp.1363-1365, Aug. 1988.
[30] Laming. R. I., Morkel, P. R., Payne, D. N., and Reekie, L., "Noise in erbium doped fibre amplifiers", *14th European Conference on Optical Communications*, Brighton U.K. Sep. 1988.
[31] Mukai, T., and Saitoh, T., "5.2-dB noise figure in a 1.5 μm InGaAsP travelling-wave laser amplifier", *Electronics Letters*, vol.23(5), pp.216-218, 1987.
[32] Olsson, N. A., "Heterodyne noise and noise measurement of a 1.5 μm resonant semiconductor laser amplifier", *IEEE Journal of Quantum Electronics*, vol.QE-22, No.5, pp.671-676, 1986.
[33] Desurvire, E., Giles, C. R., Simpson, J. R., and Zyskind, J. L., "Efficient erbium-doped fiber amplifier at a 1.53-micrometer wavelength with a high output saturation power", *Optics letters*, vol.14(22), pp.1266-1268, Nov. 1989.
[34] Nakazawa, M., Kimura, Y., and Suzuki, K., "Efficient Er(3+)-doped optical fiber amplifier pumped by a 1.48 micrometer InGaAsP laser diode", *Applied Physics Letters*, vol.54(4), pp.295-297, Jan. 1989.
[35] Mukai, T., Yamamoto, Y., and Kimura, T., "S/N and error rate perfomance in AlGaAS semiconductor laser preamplifier and linear repeater systems", *IEEE Journal of Quantum Electronics*, vol.18(10), pp. 1560-1568, Oct. 1982.
[36] Yamamoto, Y., "Noise and error rate performance of semiconductor laser amplifiers in PCM−IM optical transmission systems", *IEEE Journal of Quantum Electronics*, vol.16(10), pp. 1073-1081, Oct. 1980.

Constantinos D. Zaglanikis received the B.Eng. degree in Electronic and Electrical Engineering from University College London and he is currently working towards a PhD. at the same institution on the subject of optically controlled phase array antennas. His interests include the metaphysics of the Eastern Orthodox Church and development of a new theory which explains the quantum nature of light and matter based only on classical electromagnetism.

Alwyn Seeds received the B.Sc. and Ph.D. degrees in Electronics from the University of London. From 1980 to 1983 he was a Staff Menber at MIT Lincoln Laboratory, where he worked on millimetre-wave GaAs monolithic circuits for phased array radar. In 1983 he returned to England to take up a lectureship in Electronic Engineering at Queen Mary College, University of London and in 1986 he moved to University College London where he is now the Bell Northern Research Senior Lecturer in Opto-electronics and leader of the Microwave Opto-electronics Group. He has published some 60 papers in the fields of microwaves and opto-electronics and acted as a consultant to a number of organistions active in these areas. Dr. Seeds is a senior memeber of the IEEE, a member of the Institution of Electrical Engineers and UK Official Representative to Commision D of URSI.

MMIC PREAMPLIFIERS FOR MULTIGIGABIT-PER-SECOND OPTICAL LINKS

F. GIANNINI

DEPT. OF ELECTR. ENGINEERING
UNIVERSITY OF ROMA "TOR VERGATA"
VIA O. RAIMONDO – 00173 ROMA, ITALY

The multigigabit-per-second optical communication systems require some advanced circuital solutions in order to guarantee the inherent benefits of their use. Among the others, the receiver front end for fiber optic links, with tight constraints on bandwidth, gain, input seinsitivy and power consumption, represents a challenging task for microwave designers. On the other hand, the progressing maturity of the GaAs microwave monolithic integrated circuits (MMIC's) technology is now offering a very effective way to address these issues. The paper illustrates the present trends in this field and critically examines the already available solutions, in order to extract some design guidelines.. As an example, a realization of an advanced transimpedance front-end receiver based on some novel circuital solutions is also given.

1. INTRODUCTION

During the last few years, the improvment of Gbit/sec optical links has demonstrated to be worth of noting.

Among the others, one of the causes for the increasing attention paid to optical communication systems can be strictly related to their remarkable advantages with respect to alternative solutions based on other conventional techniques.

Lower attenuation, wider bandwidth combined with an intrinsic electromagnetic coupling immunity, low weight, size and cost are some of the interesting features of such systems [1].

Moreover, most of the presently available signal regeneration circuits (repeaters) suitable to be used in multigigabit-per-second fiber optic links, require the optical signal to be transformed in an electrical one, in order to proceed into the regeneration procedure. This is mainly due to the present availability only of few advanced prototypes for a direct optical amplification, highly attractive in order to avoid optical-electrical conversion and electronic circuitry for signal treatment, timing etc [2].

So, the classical photodiode-preamplifier solution, based on a more mature semiconductor technology, appears to be the most suitable approach to process signals at gigabit transmission rate. On the other hand, this kind of solution implies the realization of receivers in the microwave range with tight constraints on input sensitivity, overall bandwidth and gain, issues that normally appear to be conflicting ones. A particular effort is so required to find a trade-off in order to optimize the receiver performance according to its specific applications, since this circuit determines the link bit error rate (BER).

From this point of view, the progressing maturity of microwave monolithic integrated circuits (MMIC's) on GaAs have been offering very interesting solutions that appear to be extremely suitable for this kind of applications [3, 4, 5].

In fact, among their peculiar features, the reduction of parasitic reactances, with respect to the corresponding hybrid solutions and the possibility to integrate on the same chip both the photodiode and the preamplifier [6, 7, 8, 9, 10] result in an overall bandwidth enlargement and noise reduction.

Moreover, the analysis of previously proposed circuits and the corresponding experimental achievements can suggest some useful guidelines to the designer in order to perform an optimum design of an optical preamplifier in a monolithic form. In particular, taking into the proper consideration that the receiving photodiode highly affects both the bandwidth of operation of the entire optical front-end, with its junction capacitance, and the receiver sensitivity, with its noise contribution,the topology of the preamplifier to be chosen has to demonstrate a large gain-bandwidth product and a good noise performance with the lowest achievable power consumption.

2. TOPOLOGICAL SOLUTIONS

An exhaustive analysis of the front-end noise performance has been reported in the literature [1, 11] and constitutes the basis of the main preamplifier design considerations.

Starting from the minimum mean optical power level to be fed to the photodiode and fixing the required link bit error rate, the choice of the optical detector automatically determines the overall performance required from the receiver amplifier. In fact, better the photodiode, less critical is the design of the preamplifier. From this point of view, an avalanche photodetector (APD) appears to be preferable to the PIN diode solution especially for its higher optical sensitivity in the high bit rate, so reducing the effectiveness of using a very low noise preamplifier.

On the other hand, depending on their topology, the front-end preamplifiers can be divided into two groups: the classical amplifier-equalizer scheme and the transimpedance one. The first solution (Fig. 1a) offers the lowest noise level and the corresponding highest sensitivity, principally because of its high input impedance. This feature, however, causes both a limitation of the dynamic range and a dramatic "shrinking" of the overall bandwidth because of the resulting large input RC time constant. Thus an equalizer section has to be introduced to extend the receiver bandwidth up to the requested value, so compensating the integrating action of the high impedance input stage. The complexity so introduced into the receiver design and the possible degradation of the overall performance, deriving from a non-perfect pole-zero compensation between the amplifier and the equalizer stages, has been highly reducing the popularity of this solution [11].

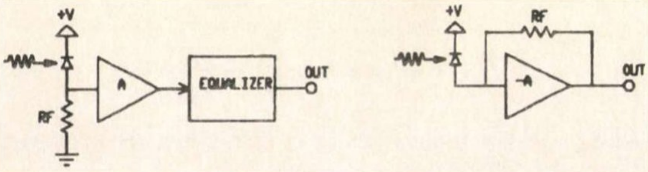

Fig. 1. a) Amplifier equalizer scheme; b) Transimpedance scheme

The transimpedance solution (Fig. 1b) avoids the problem of a reduced dynamic range. Moreover, the introduction of a negative parallel feedback, easily extends the front-end, overall bandwidth to the desired value, both enlarging the preamplifier bandwidth and reducing the RC input time constant. The corresponding sensitivity degradation, related to the thermal noise contribution of the feedback resistor, can be properly controlled with an accurate choice of the resistance value.

However, the necessity of high gain-bandwidth product, typical for the cases of optical link at very high bite rate, can require an increase in the number of the amplifying stages to be cascaded inside the feedback loop, so possibly creating some stability problems.

After all, having in mind this very important latter aspect, a transimpedance amplifier can be considered to be the best present choice for the optical front-end input stage, especially when a high sensitivity photodiode is used, so reducing the issue of a very low noise contribution from the amplifier [12].

3. TRANSIMPEDANCE AMPLIFIER

As put into evidence before, the transimpedance topology seems to be the most suitable preamplifier configuration for an optical communication receiver.

Moreover, the use, of a monolithic approach, in terms of GaAs technology, appears to be the best realization choice, even if a more complex DC coupled design is mandatory, in order to avoid the large value capacitors required to obtain a low cut-off frequency in the KHz range.

Besides the already mentioned features, like small size, low weight, lower cost for massive production, improved reliability and reproducibility are two other interesting advantages offered by the monolithic solution.

On the other hand, an increased design flexibility and a drastic reduction of the parasitic reactances assure an easier achievement of an optimized circuit solution with respect to a corresponding hybrid approach.

Taking now into considerations the basic topology of a transimpedance amplifier (Fig. 1b), it is easy to demonstrate that for a given junction capacitance C_j of the photodiode, the input resistance R_{in} of the transimpedance stage practically determines the overall bandwidth of the entire front-end.

This bandwidth, in fact, is principally related to the time constant $\tau_{\text{in}} = (C_j + C_{\text{in}})R_{\text{in}}$, where C_{in} is the input capacitance of the input stage.

The use of the lowest allowed value for the shunt feedback resistor is recommended in order to achieve the widest possible bandwidth, while preserving an acceptable noise contribution and a high overall gain.

It results that these particular features can be achieved only through the use of a high intrinsic gain "block", which in turn can be obtained only with a topological configuration involving more than a single amplifying stage. Two basic approaches are normally followed in the realization of the gain block: a simple cascade of common source stages (Fig. 2a) and a cascode configuration (Fig. 2b).

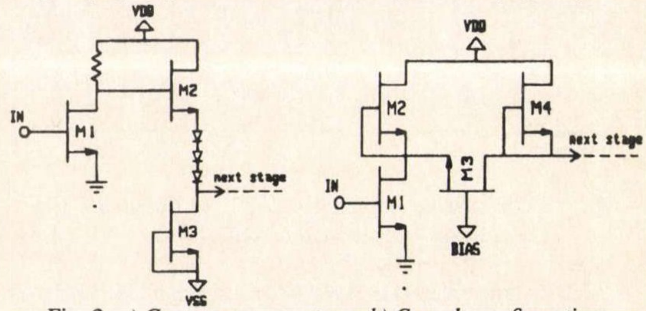

Fig. 2. a) Common-source stages; b) Cascode configuration

The first one is the most widely used configuration, especially for its lower level of complexity, as demonstrated by the many solutions presented by several authors [2, 5, 6, 13, 14, 15, 16].

The cascode configuration is a relatively new one in the field of optical receiver applications, but it appears to be extremely promising for its high gain-bandwidth product and has been receiving more and more attention [1, 3, 4, 17, 18].

A typical solution adopting a common source stage is presented in Fig. 3a, where an active load acts as a loading resistor, so improving the large signal performance and the DC power saving, while lowering the sensitivity to process variation, at the expense of only a little noise degradation. An "active" feedback is also introduced to enlarge the bandwidth, with a corresponding lowering of the gain, and a buffer level-shifting stage is added in order to reduce the next stage input capacitance loading effect. Moreover, it provides also the necessary DC voltage shifting for a correct bias of the gate of the next stage, at the expense of a typical 6 dB gain reduction. Fig. 3b shows a 2 GHz bandwidth circuit proposed by Hornbuckle [19] while Fig. 3c presents the scheme of Kolbas [7] where an output drain follower stage is introduced in order to assure a better output matching. This solution, which demonstrated to be particularly effective, has been adopted in most of the lately proposed new topologies.

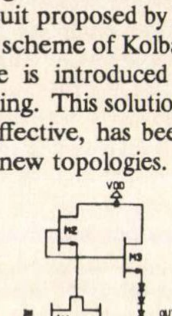

Fig. 3. a) Common-source stage with active load and feedback

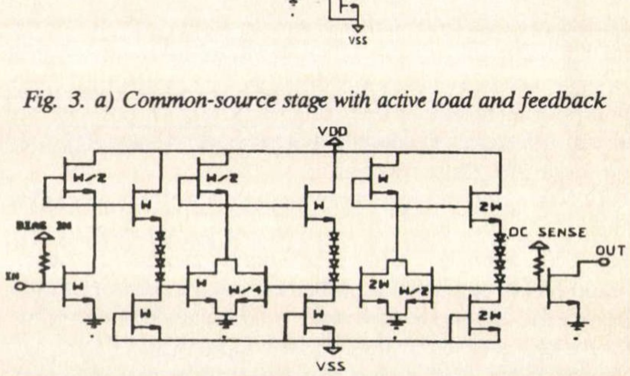

Fig. 3. b) 2 GHz bandwidth transimpedance amplifier in [19].

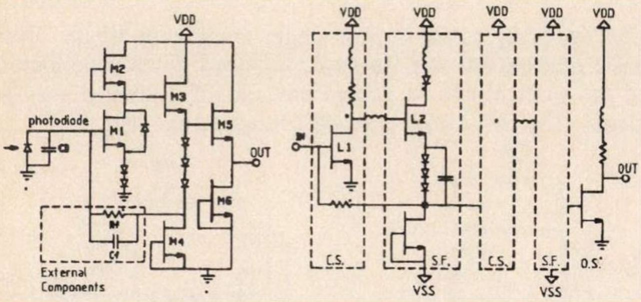

Fig. 3. c) Transimpedance amplifier in [7]; d) Transimpedance amplifier with inductor peaking in [4].

Further improvements have been proposed by Okhawa [15] introducing several "peaking" inductors to resonate the MESFET capacitances, with a corresponding increase of the overall bandwidth and an improvement of the noise performance.

Fig. 3d shows the recent solution proposed by Kikuchi [5], which includes also two kinds of peaking inductors. The gate inductor, being more sensitive to frequency response, is selected to achieve a flat response, while the drain one contributes to the band-widening, realizing the well-known "video" compensation.

A capacitor is also added in parallel to the shifting-level diode chain, creating an AC by-pass in order to avoid the frequency performance degradation due to the associated series resistances. Coplanar lines are also chosen by the authors to reduce the coupling between adjacent lines.

Besides some performance degradation in the practical realization, principally related to the poor frequency behaviour of the spiral incductors, due to their stray capacitances, a 57 dBohm transimpedance gain up to 8.5 GHz with an input noise current of $20.9pA/\sqrt{\mathrm{Hz}}$ from DC to 7 GHz were demonstrated, using a .3 μm MESFET gate technology and a PIN diode as a photodetector [5].

The cascode configuration seems to be extremely attractive for high speed optical communication systems, due to the several advantages offered by this topology with respect to the common source one. As it was seen before, in fact, the shunt feedback is typically applied around a "single" stage, limiting the gain- bandwidth product of the entire amplifier. It is well known, however, that the gain can be increased cascading several of such stages, even if it results in a remarkable bandwidth shrinkage. Otherwise, if no bandwidth degradation is accepted, it is necessary to apply the feedback to a multi-stage higher gain block. With the common source configuration, the request of an overall high open-loop gain can be addressed only cascading at least three common source inverting stages, due to regenerative behaviour of a two-stage configuration. Also in this case, however, the presence of a global input-output feedback can introduce severe stability problems, possibly out of the operating bandwidth, because of the accumulated input-output phase rotation.

The cascode configuration a single inverting (common source) — non inverting (common base) two stage amplifier, overcomes this kind of problems. Moreover, the reduced Miller capacitance of the first common-source stage, due to the low input resistance of the cascoded common-base stage, assures a considerable enlargement of the overall bandwidth. The input capacitance of the cascode stage, in fact, can be expressed (see Fig. 2b) as

$$C_{\mathrm{in}} \simeq C_{gs} + C_{gd}\left(1 + \frac{g_{m1}}{g_{m3}}\right) \tag{1}$$

with g_{m1}/g_{m3} usually close to 1. Moreover, the total gain of the amplifier can be expressed as

$$G_{\mathrm{casc}} = -\frac{g_{m1}}{g_{d4}} \cdot \frac{1}{1 + (g_{d1} + g_{d2})/g_{m3}(1 + g_{d3}/g_{d4})} \tag{2}$$

where g_{mi} and g_{di} are the transconductance and the drain conductance of the $i-th$-MESFET respectively. With a proper choice of the gate width of the various MESFET's, so fully utilizing the unique flexibility that the monolithic approach offers, a gain-bandwidth product significantly higher than that provided by the common-source configuration can be obtained. A first example of an application of a cascode to an optical front-end was proposed by Bahl [3] and it is reported in Fig. 4a. A .5 μm technology was used and a PIN diode adopted as photodetector. In particular, with a feedback resistor of about 2 Kohm, a transimpedance gain of 64 dBohm across a 1.6 GHz bandwidth was achieved with an input sensitivity of -28 dBm, while assuring a 30 dB dynamic range. More recently Colleran [4] presented the scheme of Fig. 4b, where two transimpedance cascode stages with an "active" feedback are cascaded, while a simple common drain assures the necessary 50 ohm output matching. Using a standard 1 μm MESFET technology a voltage gain of 26 dB and a bandwidth of 3.2 GHz were obtained with a noise figure ranging from 6 to 8 dB across the entire band.

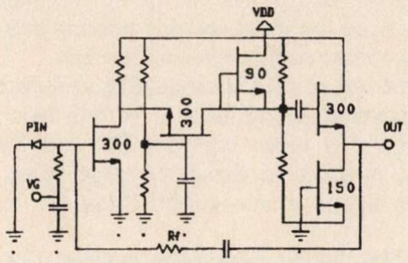

Fig. 4. a) Cascode amplifier proposed in [3].

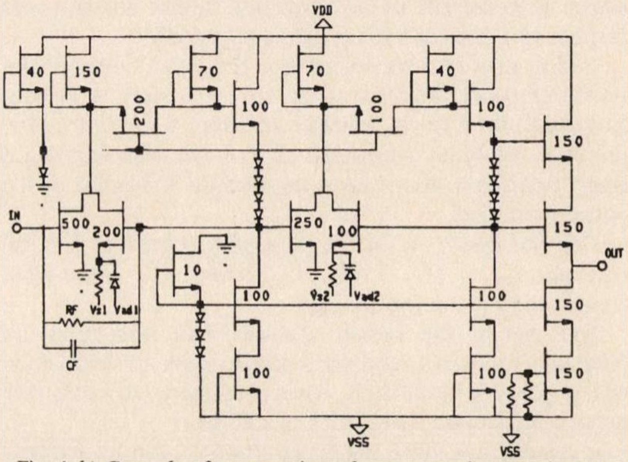

Fig. 4. b) Cascade of two transimpedance cascode stages in [4].

Finally, two different applications of the well known "feed-forward" technique have been demonstrating the suitability of this approach for the realization of improved MMIC's transimpedance amplifiers (Fig. 4c, 4d).

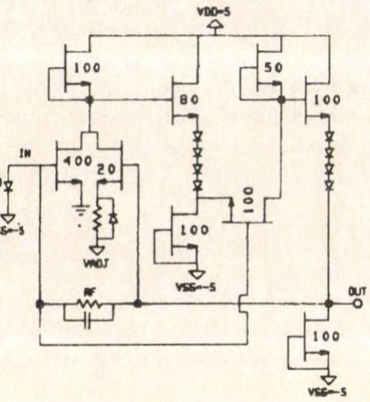

Fig. 4. c) Feed-forward technique propsed in [1] and [17].

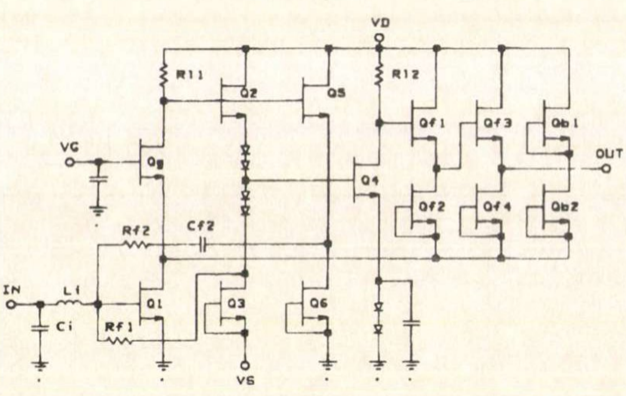

Fig. 4. d) Transimpedance amplifier with three feedback loops in [22].

More precisely with the topological solution of Fig. 4c, which has been proposed by Mauri [1] a flat in-band transfer function has been obtained, through a phase shift reduction obtained reintroducing the input signal in the gate of the common gate MESFET. A decoupling buffer stage inserted in the cascode stage between the common source and the common gate, represents another interesting circuital solution. This stage, in fact, provides the proper bias voltage level to the common-gate stage, while decoupling the drain of the common-source MESFET, so avoiding the inherent gain degradation. A consequent sharp peaking in the frequency behaviour related to an existing potential instability region (where $|S_{11}| > 1$), can be controlled and totally eliminated by a proper design of the "feed-forwarding" technique.

A 2.8 GHz bandwidth with a gain of 57 dBohm, an input noise current of $6pA/\sqrt{Hz}$ at 1 GHz and sensitivity of -35 dBohm for 10^{-9} BER, with a power consumption of 900 mW are the most interesting features of this 1 μm technology achievement.

Fig. 4d shows a novel circuit solution utilizing three different feedback loops [22]. The 1.5×1.5 mm^2 chip realization, resulted in a 3 dB bandwidth of 13 GHz with 55 dBohm transimpedance gain and a noise current contribution less than $15pA/\sqrt{Hz}$ all over the bandwidth. The improved features are mainly due to one of the three loops, which has been designed in order to supply a negative feedback current that becomes positive at high frequencies, using the extra-phase delay of the input cascode stage. Moreover, the combined effect of the input matching network and the RC feedback loop compensates both the diminishing real part of the input impedance of the cascode stage, that highly affects the high frequency behaviour of $|S_{11}|$, and the increasing effect of the input capacitance, that mantains $|S_{11}|$ still large at higher frequencies. An $|S_{11}|$ close or better than -10 dB in the entire bandwidth is so achieved.

4. DESIGN CONSIDERATIONS

On the basis of the previously discussed results and the critical analysis of the topologies previously reported in the literature, the cascode-based transimpedance amplifier seems to be the most promising solution or an optical amplifier front-end. Moreover, the same analysis can suggest some useful guidelines to optimize the electrical performance of this component. Apart some peculiar aspects, including some minor but very useful circuit solution (bypass capacitors, peaking inductors etc.) in fact, most of the proposed topologies practically consist of the cascade of three main functional blocks:

- an input "true" transimpedance stage, which has to convert the photodiode current into a voltage signal, while assuring both a minimum noise level contribution and the required input matching;
- an intermediate stage to provide a further enhancement of the voltage gain, to meet the overall gain specification for the entire front-end, while avoiding a significant reduction of the overall bandwidth;
- an output stage which has to assure the proper 50 ohm output matching.

Each of three sections, so specified into a basic topology, should be separately optimized in order to assure, to the entire circuit, the requested level of performance, taking into consideration some other peculiar requirements. This is the case, for instance, of the power consumption that is normally required to be as low as possible, according to some specific use which the integrated front-end is devoted to.

The input stage topology, can be a "classical" transimpedance one. It means that the designer has to choose the gate width of two MESFETs, their biasing point and the related biasing network, the two drain loading and, finally, the feedback resistor.

As it was pointed out, this stage has to guarantee principally the requested bandwidth and sensitivity. A resistive loading for the first MESFET, a biasing network with the resistance values at the highest acceptable value, for instance, keeps the noise contribution at the lowest level, while the feedback resistor value derives from a trade-off between the desired bandwidth and, again, the noise contribution. The biasing point of the first MESFET and its gate width, chosen in order to give an input capacitance roughly equal to the photodiode junction one [20], finally assure the requested front-end sensitivity. Less critical, from this point of view, appears the design of the gate widths for the common-gate stage and its active load, that can be chosen in order to maximize the gain-bandwidth product according to Eq. (1) and (2).

The second block of the whole front-end, can be a single voltage amplifier, properly designed to rise the gain without a dramatic change in the overall bandwidth. From this point of view, another cascode stage for instance [4], has demonstrated to be effective. On the other hand an interesting alternative, can be offered by the composite amplifier of Fig. 5. [18]. The stage, corresponding to a voltage follower driving a non inverting common-stage, can be also seen as a MESFET differential pair with the drain on one side connected directly to the supply, so doubling the differential to single-ended gain with respect to the symmetric differential pair [21]. In particular, with a proper choice of the various elements, this solution assures practically the same gain-bandwidth performance as a corresponding cascode topology.

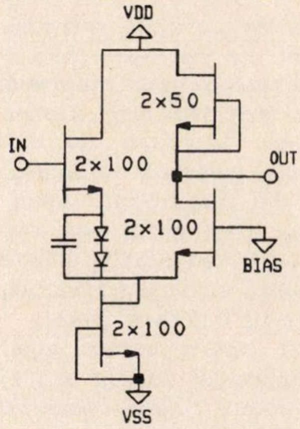

Fig. 5. Asymmetric differential pair.

Moreover, the circuit shown in Fig. 5. offers a very important intrinsic buffering function, extremely useful in the design procedure, allowing a separate optimization of the preceding transimpedance section, while introducing the requested voltage level-shifting in order to fix a correct biasing point for the common-gate stage.

Finally, the third block of the amplifier, i.e. the output matching section can be realized with a simple source follower stage.

In this case, a MESFET with a transconductance of 20 mA/V normally assures the required $|S_{21}|$ with a consequent reduction of 6 dB gain. Moreover, this stage normally dissipates a large part of the total amount of DC power dissipated by the entire front-end [6, 15].

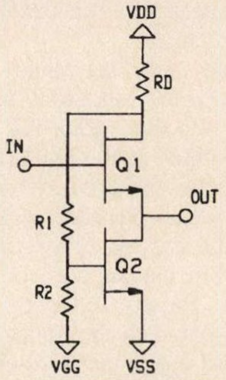

Fig. 6. Composite source follower.

Fig. 6. shows an interesting alternative to the single voltage follower that corresponds to a composite amplifier having improved performance, principally from the point of view of the power consumption.

More precisely, the first MESFET provides also an inverted output from its drain that is applied to a second inverting stage that provides an additional output to reinforce the output of the first stage. Some easy calculations demonstrate that, at lower frequencies, the composite source follower behaves like a single source follower showing an effective transconductance

$$Gm_{\text{eff}} = g_{m1}\left[1 + g_{m2}R_d\frac{R_S}{R_1 + R_2}\right] \tag{3}$$

and an effective output resistance

$$R_{\text{out}} = \frac{1}{Gm_{\text{eff}}} \tag{4}$$

With a proper choice of the two transistors and the resistors, the desired level of Gm_{eff} can be obtained, so reducing the power dissipated, according to the use of two smaller MESFETs.

As a result of the previously outlined design guidelines, a scheme of a newly proposed optical preamplifier is indicated in Fig. 7a, where a very simple configuration was chosen, in order to maximize the yield in the realization phase. The input section is a classical transimpedance stage. Its second section is a modified differential pair and the output one a common drain stage. From the simulated performances (using the Plessey F20 MMIC process), a bandwidth of 2.3 GHz, including the .3pF diode capacitance, and a transimpedance gain of about 70 dBohm results, with an output matching better than -13dB, a power consumption of about 700 mW and an input noise equivalent current less than $7pA/\sqrt{Hz}$. Also a high stability level is assured. Fig. 7b shows a microphotograph of the realized circuit (chip size $1.8 \times 1.8\text{mm}^2$), while Fig. 7c shows the simulated and measured transimpedance gain for three different chips from the same wafer. The measurements were performed without the photodiode and a transimpedance gain of 67 dBohm in a 2.5 GHz bandwidth was demonstrated. Fig. 7d and 7e report from the same realization the simulated and measured equivalent noise current vs. frequency with the temperature $(-20, +50°\text{C})$ as a parameter. A typical power consumption of 610 mW was measured.

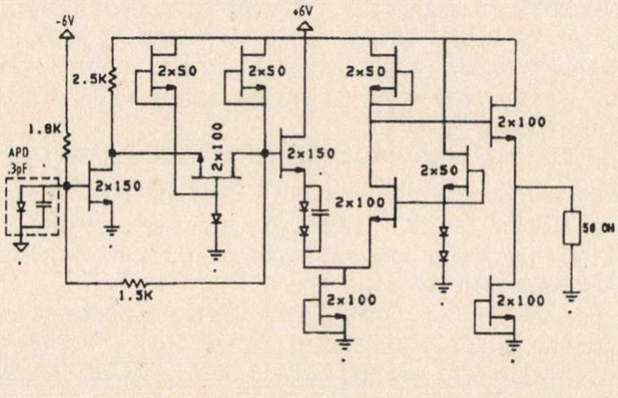

Fig. 7. a) Schematic of the first MMIC optical preamplifier.

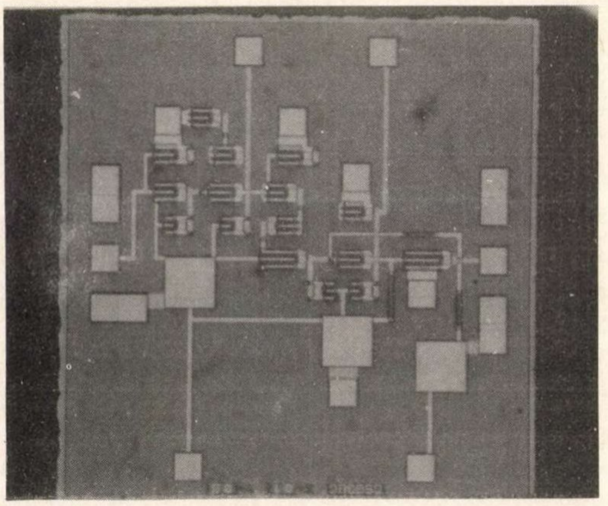

Fig. 7. b) Microphotograph of the first MMIC optical preamplifier.

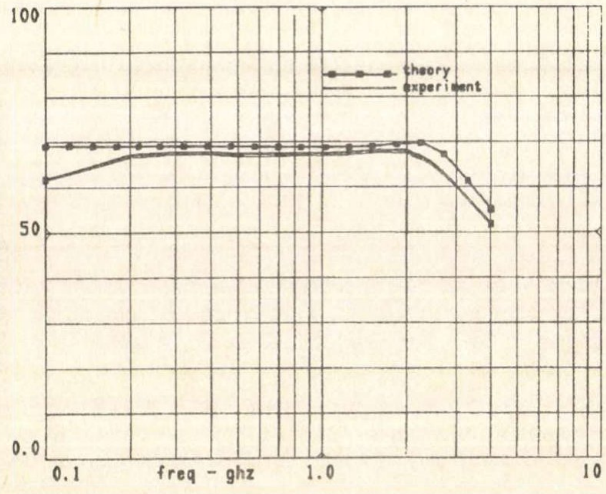

Fig. 7. c) Simulated and measured transimpedance gain.

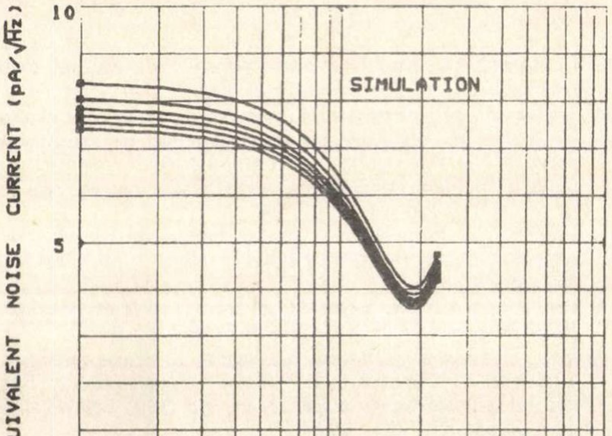

Fig. 7. d) Theoretical temperature behaviour (−20, +50° C) of the equivalent input noise current density vs frequency

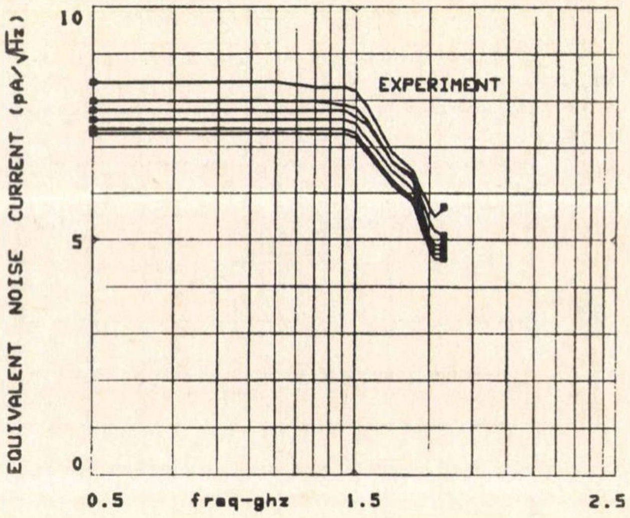

Fig. 7. e) Experimental temperature behaviour (−20, +50° C) of the equivalent input noise current density vs frequency.

Finally, Fig. 8. shows a series of new circuit configurations introduced in the previous scheme to enlarge the bandwidth and to improve the other important features. As it is easy to see, the input transimpedance section is exactly the same as in Fig. 7a. The differential pair is now modified by introducing a "composite" source follower stage with reduced gate width so improving both the DC power consumption and the "buffering" performance of the stage. A drain peaking inductor, with 5 turns, further increases the bandwidth. The output buffer stage has been designed according to the same philosophy.

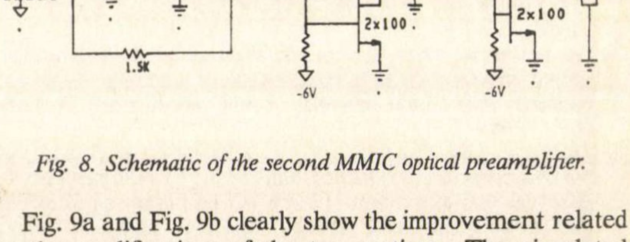

Fig. 8. Schematic of the second MMIC optical preamplifier.

Fig. 9a and Fig. 9b clearly show the improvement related to the modifications of the two sections. The simulated results, obtained including all the parasitics of the various elements, give a bandwidth of 3.5 GHz, including the .3pF diode capacitance, with a 70 dBohm gain, an output matching better than -15 dB across the entire bandwidth and a DC power consumption less than 500 mW.

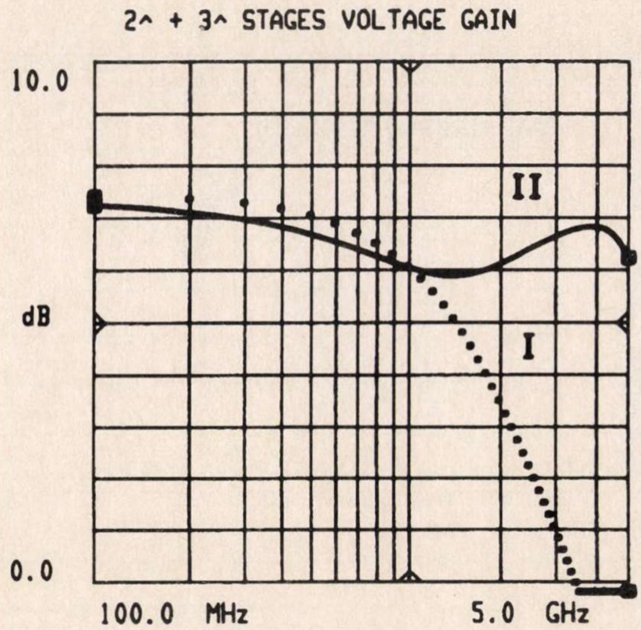

Fig. 9. a) Comparison of differential pair and output buffer cascade performance in the first and second design.

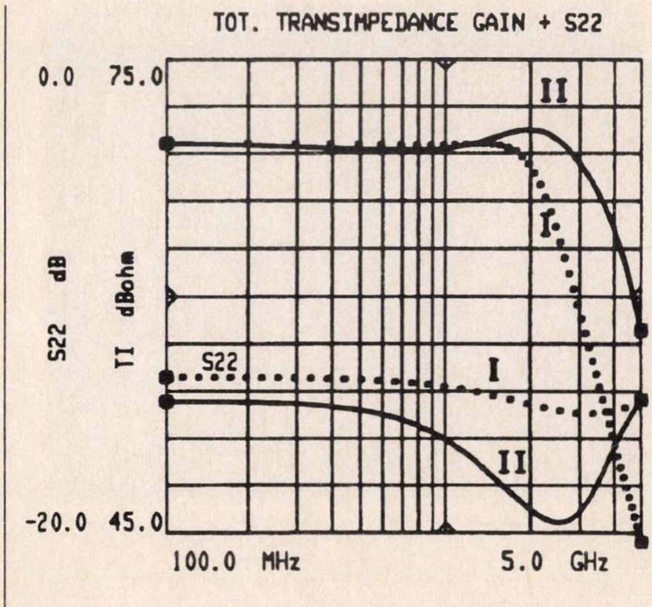

Fig. 9b Comparison of transimpedance gain and S_{22} of the first and second design.

5. CONCLUSIONS

The MMIC technology seems to be an effective solution for the realization of advanced very wideband optical preamplifiers.

A proper design of the various sections that constitute a typical optical front-end, assures both a good level of input sensitivity and a high gain-bandwidth product.

From this point of view, a transimpedance topology seems to be the most suitable preamplifier configuration, while the cascode solution assures several advantages with respect to the often used common-source one.

Finally, some interesting new circuit solutions demonstrate the possibility to further improve some already established topologies, with respect to both the gain-bandwidth performance and the DC power consumption.

REFERENCES

[1] Mauri, A., Bastida, E. M., Chiappa, P. A., Donzelli, G. P., Feudale, M., "High performance GaAs monolithic transimpedance amplifiers for multigigabit per second fiber optic links", *Gallium Arsenide Apllication Symposium*, pp.367, Rome, Apr.1990.

[2] Archambault, Y., Pavlidis, D., Guet, J. P., "GaAs monolithic integrated optical preamplifier", *Journ. of Lightwave Tech.*, vol.lt–5, no.3, March 1987.

[3] Bahl, I., Griffin, E., Powell, W., Ring, C., "A ligh speed GaAs monolithic transimpedance amplifier", *IEEE Microwave and Millimeter-wave Monolithic Circuits Symposium*, pp.35–38, 1986.

[4] Colleran, A., Abidi, A., "A 3.2 Ghz 26dB wide-band monolithic matched GaAs mesfet feedback amplifier using casodes", *IEEE Trans. on MTT*, vol.36, no.10, pp.1377-1385, Oct. 1988.

[5] Kikuchi, H., Miyagawa, Y., and Kimura, T.,"Broadband GaAs monolithic equalizing amplifiers for multigigabit-per-second optical receivers", *IEEE MTT-S Digest*, pp.785-788, 1990 and IEEE Trans. on MTT, vol.38, no.12, pp.1916-1922, December 1990.

[6] Harder, C.S., Zeghbroeck, Van., Meier, H., Patrick, W., and Vettiger, P., "5.2 GHz bandwidth monolithic GaAs optoelectronic receiver", *IEEE Electron Device Letters*, vol.9, no.4, pp.171-173, April 1988.

[7] Kolbas, R. M., Abrokwah, J., Carney, J. K., Bradshaw, D. H., Elmer, B. R., Biard, J. R., "Planar monolithic integration of a photodiode and a GaAs preamplifier", *Appl. Phys. Lett* 43(9), pp.821-823, 1th Nov. 1983.

[8] Ito, M., Wada, O., Nakai, K., Sakurai, T., "Monolithic Integration of a metal-semiconductor-metal photodiode and a GaAs preamplifier", *IEEE Electron Device Letters*, Dec. 1984.

[9] Rogers, D. L., "Monolithic integration of a 3-GHz detector/preamplifier using a refractory-gate, ion-implanted mesfet process", *IEEE Electron Device Letters*, Nov. 1986.

[10] Makikuchi, M., Hamagichi, H., Kumai, T., Aoki, O., Oikawa, Y., Wada, O., "GAInAs pin photodiode/GaAs preamplifier photoreceiver for gigabit-rate communications systems using flip-chip bonding techniques", *Electronics Letters*, vol.24, no.16, pp.995-996, 4th Aug. 1988.

[11] Muoi, T. V., "Receiver design for high-speed optical fiber systems", *Journ. of Lightwave Tech.*, vol.LT-2, no.3, pp.243-267, June 1984.

[12] Personik, S. D., "Receiver design for optical fiber systems", *IEEE Proc.*, vol.65, no.12, pp.1670-1678, Dec 1977.

[13] Imai, Y., Kato, N., Ohwada, K., Sugeta, T., "Design and preformances of monolithic GaAs direct-coupled preamplifiers and main amplifiers", *IEEE Trans. on MTT*, vol.MTT-33, no.8, pp.686-692, Aug. 1985.

[14] Hamaguchi, H., Makiuchi, M., Kumai, T., and Wad, O, "GaAs optoelectronic integrated receiver with high-output fast-response characteristics", *IEEE Electron Device Letters*, vol.edl.8, no.1, pp.39-41, Jan. 1987.

[15] Ohkawa, N., "Fiber optic multigigabit GaAs MIC front-end circuit with Inductor Peaking", *Journ. of Lightwave Tech.*, vol.6, no.11, pp.1665-1671, Nov. 1988.

[16] Ishihara, N., Kikuchi, H., Ohara, M., "Gigahertz-Band High-Gain GaAs Monolithic amplifiers using parallel Feedback Technique", *IEEE Journal of Solid State Circuits*, vol.24, no.4,

pp.962-968, August 1989.

[17] Mauri, A., Bastida, E. M., Chiappa, P. A., Feudale, M., "Very high performance d.c. coupled MMIC FET amplifiers", *Proceed. of 20th Eu.M.C.*, vol.2, pp.1761-1765, 1990.

[18] Giannin, F., Paolini, C., Orengo, G., "Advanced MMIC Preamplifier for Optical System", *Proceed. of 3rd Workshop on GaAs in Telecommunications*, Milano, pp.105-116, April 1991.

[19] Hornbuckle, D. P., Van Tuyl, R. L.: "Monolithic GaAs direct-coupled amplifiers", *IEEE Trans. on Electron Devices*, vol.ED-28, no.2, pp.175-182, Febr. 1981.

[20] Minasian, R. A., "Optimum design of a 4-Gbit/s GaAs mesfet optical preamplifier", *Journ. of Lightwave Tech.*, vol.LT-5, no.3, pp.373-379, March 1987.

[21] Abidi, A. A., "On the operation of cascode gain stages", Regular Correspondence, *IEEE Journal of Solid-State Circuits*, vol.23, no.6, pp.1434-1437, Dec. 1988.

[22] Imai Yuhki, Sano Eichi and Asai Kazuyoshi, "Design and perfomance of wideban GaAs MMIC's for high-speed optical communication systems", *IEEE Trans. on Microwave Theory and Techniques*, vol.40, no.2, Feb. 1992.

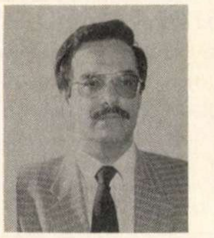

Franco Giannini received the (summa cum laude) degree in Electronics Engineering, from the University of Roma "La Sapienza" in 1968, with a graduation thesis on GaAs epitaxial growth and device fabrication techniques. In 1968 he joined the Institute of Electronics of "La Sapienza", where he was Assistant Professor until 1980. He was Associate Prof. of Microwaves at the University of Ancona, Italy (73−74), and of both Solid-State Electronics (74−77) and Applied Electronics (77−80) at the University of Roma "La Sapienza". In 1980 he became Full Professor of Applied Electronics at "La Sapienza". Since 1981 he has been with the II University of Rome "Tor Vergata". He has been working on problems concerning theoretical characterization and design methodologies of active and passive microwave components and circuits, including GaAs monolithic circuits. He chaired the theme, "Monolithic Integrated Circuits in the 20-30 GHz Range", of the national project. "Solid State Electronic Material and Devices", of the Italian National Council for Research and he is active in the European Community ESPRIT Projects. He is also a member of the European Working Group for GaAs Microelectronics as an official representative of the Italian Ministry of Scientific Research. Franco Giannini is author or co-author of more than one hundred and forthy technical papers, including numerous articles in the IEEE Transactions on Microwave Theory and Techniques, International Journal of Satellite Communications, Space Communications and Broadcasting, Alta Frquenza, and the IEEE International Microwave Symposium and European Microwave Conference Proceedings. He has been chairman and co-chairman of various Internatinal Symposia on GaAs, on Microwave and Millimeter Wave Techniques Applications and is a member of some Technical and steering Comittees of European Scientific Conferences. Prof. Giannini is a consultant for various national and international industrial and governemental organizations, and a senior member of IEEE.

AN OPTICAL LINK FOR THE TRANSMISSION OF MICROWAVE SIGNALS

S. TEDJINI and N. EL KAMOUN

LEMO URA CNRS 833,
23 AVENUE DES MARTYRS, BP 257
38016 GRENOBLE, FRANCE

The paper deals with the microwave matching of optoelectronic devices. A comparative theoretical study of several matching techniques is reported. An optical link at $0.8\mu m$ for the optical transmission of microwave signals around 2 GHz is realized and characterized. It uses commercially available optoelectronic components: Sharp LT022MS laser diode and Mitsubishi APD PD1002 photodetector. We show that an efficient microwave matching of the optoelectronic elements can reduce significantly the insertion loss even for optoelectronic devices not optimized for high frequency ranges. The realized optical link shows 0.58 dB power gain at 2.08 GHz and a -3 dB bandwidth better than 14 %.

1. INTRODUCTION

Optical links at microwave frequencies are circuits of great interest for microwave applications. Today, optical links are increasingly used to replace conventional microwave solutions for the transmission of RF signals and more recently for optical processing of microwave signals [1,2]. The advantages of optical links are mainly due to the characteristics of both the optical fibers and the optical channel. Practically the single mode optical fiber at 1.3μm is unlimited in bandwidth and losses are < 0.5 dB/km. Unfortunately, these advantages are masked by the electrical to optical (emitter) and the optical to electrical (receiver) transducers.

Two types of optical links exist: the directly modulated optical link, which uses a directly modulated laser diode as transmitter, and the externally modulated one, which uses a light source and an external modulator. A comparison between the two types of links has been reported by several authors and the estimated insertion losses (for the RF signal) are 20 to 50 dB for directly modulated links and 30 to 60 dB for externally modulated links [3].

Several attempts have been reported in the literature to minimize the insertion loss of optical links. They mainly consist of efficient microwave impedance matching and optimization of the driving circuits for the two transducers. The best performance (a power gain of 0.13 dB at 3 GHz) is found in the literature for a directly modulated link at 1.3μm using optimized non commercially available transducers and RF mounts [4]. In the first part of this paper, we present and compare several purely reactive matching circuits for laser diode which ensure a maximum transmission. We report, in the second part, a 0.58 dB power gain directly modulated 0.8μm optical link operating around 2 GHz. This link shows, a -3 dB bandwidth in the order of 14 %. It has been realized with commercially available transducers: Sharp LT022MS laser diode and Mitsubishi APD PD1002 photodetector.

2. ELECTRICAL MODELLING OF OPTOELECTRONIC DEVICES

The first step when dealing with the RF matching of an optoelectronic device is the determination of its equivalent electrical network. This is a classical procedure for microwave devices. It can be achieved using a Vector Network Analyser (VNA) and a CAD software. First, the scattering parameters (S parameters) of the device under study are measured. In the experimental characterization we have used the HP8510B Analyser. Then, using a realistic electrical model of the device under study, the values of the elements of the equivalent circuit are obtained by fitting the values of the S parameters of the model to the measured ones. This step is usually performed with the help of a CAD software. In his study the HP-Microwave Design System (MDS) software [5] has been used.

As an example of this procedure we apply it to a 1.3μm chip laser diode. The extracted equivalent circuit is given in Fig. 1. The diode has a nominal impedance of 2Ω. The series inductance L is mainly due to the bonding wire (typical value 1 nH/mm), while the parallel capacitance is due to the diffusion capacitance of the laser diode (few pFs) and R1 is the series contact resistance. This is due to the chip configuration on the experimented laser diode.

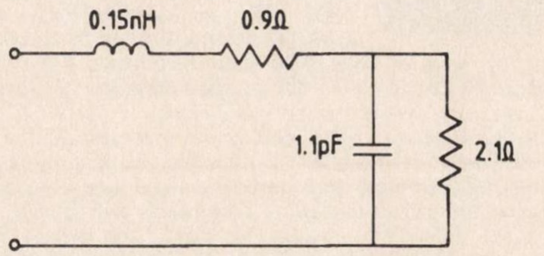

Fig. 1. Equivalent circuit model for the laser diode

3. MICROWAVE MATCHING OF OPTOELECTRONIC DEVICES

Each optoelectronic device can be modelled by its equivalent electrical network. The matching operation consist of calculating a two-port microwave network which will realize the connection between the input or output microwave line of interest and the optoelectronic device.

Such a matching network must provide a maximum transmission between the microwave line and the optoelectronic device. The technique currently used to match the laser diode to the 50Ω standard is to introduce a series resistance to bring up the total termination impedance to 50Ω. As a consequence, the power absorbed by the laser diode is only few % of the total driving power. This technique is quite easy to perform but the efficiency is very poor. In order to avoid this disadvantage, the matching circuit must be lossless and calculated in such a way that its input reflection coefficient is extremely low. Several circuit topologies are possible in practice which can be divided into two classes depending on the expected frequency response.

3.1. Narrow Band Matching

Two techniques can be considered in this case. The first one uses a quarter wave ($\lambda/4$) transformer which simply connects the optoelectronic device to the input line. Given the equivalent impedance (Z_e) of the optoelectronic device, the characteristic impedance (Z_c) of the feed line and (Z_r) of the transformer line; the matching at a frequency (f_0) is achieved if we realize the condition $Zr = \sqrt{(Z_c \cdot Z_e)}$ under the assumption that the impedance (Z_e) is purely active. In the general case of complex impedance ($Z_e = |Z_e| \exp(j\beta)$) the previous relation becomes $Z_r = \sqrt{(Z_c.|Z_e|\cos(\beta)}$ and we must add a lumped or distributed reactance at the input of the transformer in order to cancel the total reactance. Another way in the case of complex impedance (Z_e) consist of cancelling its reactive part by adding the needed reactance before the use of the $\lambda/4$ transformer. Fig. 2. gives an example of this technique.

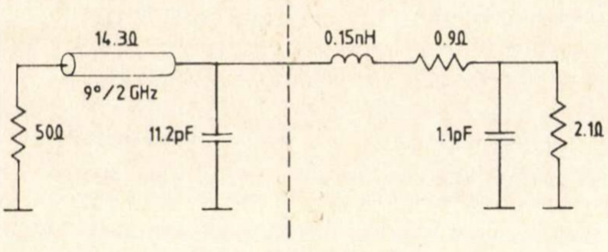

Fig. 2. One section matching impedance

The second matching method is the classical "stub" technique. By using a transmission line of length "l" and characteristic impedance "Z_c" we transform the impedance "Z_e" of the device under study into an impedance having Z_c as real part. The imaginary part of this transformed impedance is cancelled by adding, in parallel, a stub. This technique is used in Fig. 3.

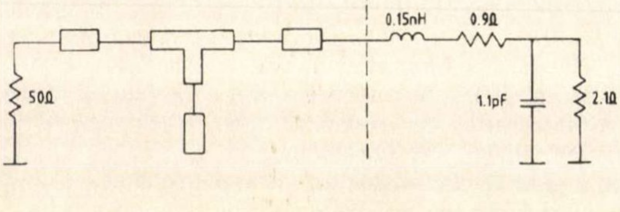

Fig. 3. Single matching stub

The previous techniques have been applied to match the laser diode modelled in Section 2. In the first case the obtained insertion loss is less than 1.6 dB for 6.5 % bandwidth around 2 GHz. In the second case, for the same insertion loss, the obtained bandwidth is 4 % around 2 GHz. The reflection coefficient is better than 25 dB in the two cases which corresponds to a very good matching of the laser diode but the bandwidth is quite narrow. larger bandwidth can be obtained if we accept higher VWSR. As an example the relation between the bandwidth ($\triangle f/fo$) and the VWSR (ρ) in the case of $\lambda/4$ transformer technique is given by:

$$\rho = 1 + \frac{\pi}{2}\frac{(Z_r - R)}{\sqrt{RZ_r}}\frac{\triangle f}{f_0}$$

where R is the real part of Z_e, Z_r is the characteristic impedance of the $\lambda/4$ transformer line.

3.2. Wideband Matching

In order to enlarge the bandwidth we must reduce the frequency selective behaviour of the matching circuit. Several techniques are found in the literature. In this study we consider two classical techniques and we introduce a new one.

3.2.1. Multisection transformer

The multisection technique (Figs. 4. and 5.) is one of the most efficient wide band matching methods. Its main advantage consists of avoiding a high discontinuity between two successive sections. This property is particularly important when dealing with components having low input impedance such as laser diodes. As an example, for two $\lambda/4$ transformers the approximated expression of the VWSR (ρ) for a bandwidth ($\triangle f$) around the central frequency (f_0) is given by:

$$\rho = 1 + \left(\frac{\pi}{2}\right)^2 \frac{(Z_r - R)}{\sqrt{RZ_r}}\left(\frac{\triangle f}{f_0}\right)^2$$

Comparing this expression with the one describing the single section transformer we remark that for the same value of the VWSR the obtained bandwidth is significantly enhanced in the case of the two section transformer.

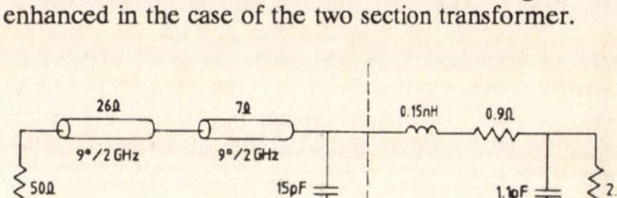

Fig. 4. Two sections matching impedance

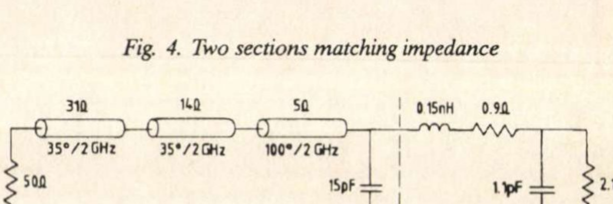

Fig. 5. Three sections matching impedance

Applying this technique to the previous laser we obtain that for insertion loss less than 1.6 dB, the bandwidth is better than 18 % for the two sections transformer and 48 % in the case of the three sections transformer.

3.2.2. Continuous exponential section

Instead of the use of several sections the bandwidth may be significantly enhanced if we use a progressive taper as shown Fig. 6. The progressive taper is the limiting case of an infinite number of multisection transformers. However, the use of an infinite number of $\lambda/4$ sections leads to an infinite length of the matching circuit which is impossible from the practical point of view. To obtain a finite length we use the properties of the continuous taper. The performance of such a matching circuit will depend on its length and its longitudinal profile. The exponential profile seems to be one of the good choices for the laser diode. The application of this technique to the laser diode under study results in a 60% bandwidth around 2 GHz for an insertion loss of 1.6 dB.

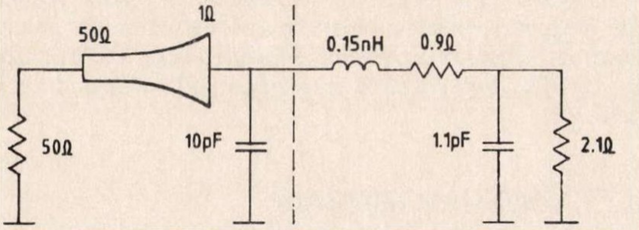

Fig. 6. Tapered transmission lines

3.2.3. Matching Filter

The microwave filter can be considered as a matching circuit too. Either lumped or distributed configurations are suitable. The main advantage of this technique is its very flat response in the filter bandwidth. To match the laser diode under study, we begin by cancelling the reactive part of its impedance at the central frequency. This can be done by adding, in series or in parallel, an adequate lumped or distributed reactance. Then, we synthesize the microwave filter in such a way that its input impedance is 50Ω. The application of this technique to the considered laser diode gives the filters shown in Figs. 7. and 8. These two configurations has been optimized using the MDS-HP software. The distributed filter uses microstrip technology. The stimulated results of the two matching filters show that insertion losses are less than 1.6 dB for 50 % bandwidth around 2 GHz for the lumped element filter and 51 % in the case of the distributed element filter.

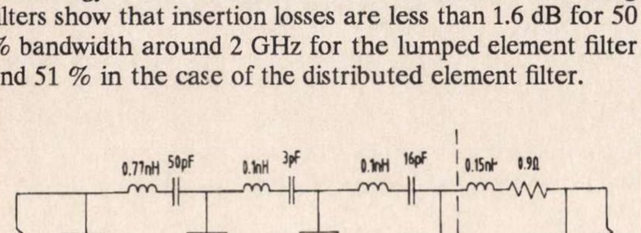

Fig. 7. Structure of the lumped elements band-pass filter

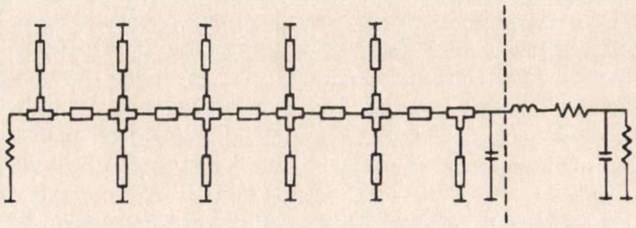

Fig. 8. Structure of the distributed elements band-pass filter

Finally we report in the table below a comparison of the previous matching techniques applied to the laser diode modelled in Section 2.

Table 1. Comparison of matching techniques

	One $\lambda/4$ section	Two $\lambda/4$ sections	Three $\lambda/4$ sections	Expo-nential taper	Stub	Lumped filter	Distri-buted filter
Reflection coefficient dB at 2 GHz	-45	-21	-19	-15	-50	-22	-15
Insertion losses dB <	1.6	1.6	1.6	1.6	1.6	1.6	1.6
Band-width %	6.5	18	48	60	4	50	51

4. APPLICATION

This section gives the experimental results obtained for an optical link using the Sharp LT0222MS laser diode and the Mitsubishi avalanche photodetector PD 1002. Microwave characteristics for the laser diode and photodiode were measured with a network analyzer (HP8510). For determination of their equivalent circuits the HP-MDS software has been used. The models are given in Fig. 9.

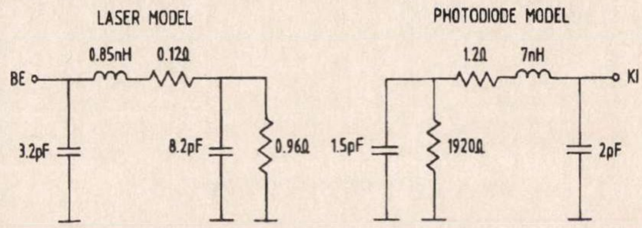

Fig. 9. Electrical models used for laser diode and photodiode

The electrical models of the two previous optoelectronic components have been used to calculate and optimize the DC driving and the microwave matching circuits around 2 GHz. A lumped reactance and a one section transformer have been used to realize the matching of the laser diode. A distributed reactance (stub) and a transformer line have been used to match the photodetector. Then, the overall performance of an optical link using these optoelectronic components has been simulated using HP-MDS software. In this simulation, we assumed a direct illumination of the photodetector by the modulated optical signal emitted by the laser diode. The dynamic current gain of the optical link is given by the product of the quantum efficiencies of the laser diode and the photodetector. Since the latter is an avalanche type the current gain will strongly depend on the DC driving voltage.

The matching circuits of the two elements have been realized on Epsilam 10 substrate. The diodes have been fixed on an optical bench and a lens has been placed between the laser diode and the photodetector to focus the optical signal on the photodiode. For the experiments, the distances between the three elements: laser diode, photodiode and lens as well as their alignment have been optimized manually.

The static characteristic of the realized optical link, which gives the detected photocurrent as a function of the laser diode current, is given in Fig. 10. The slope of the curve gives the dynamic current gain (the quantum efficiency) of the link. The best result (0.3) is obtained for a DC voltage of the photodiode in the order of 115 V.

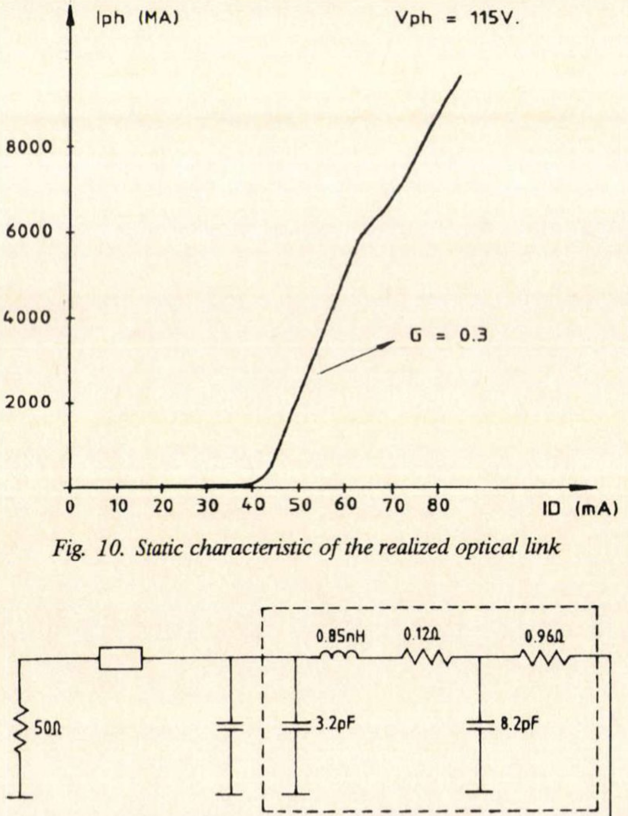

Fig. 10. Static characteristic of the realized optical link

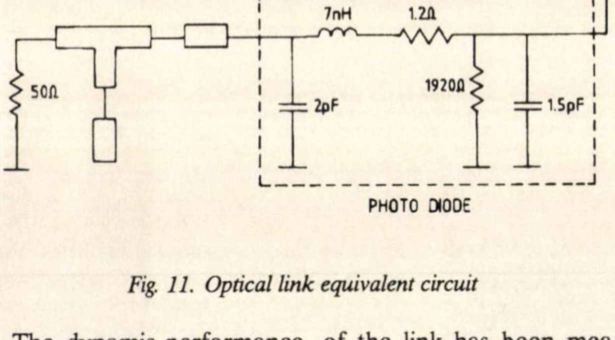

Fig. 11. Optical link equivalent circuit

The dynamic performance, of the link has been measured under 115 V DC of photodiode voltage. The measured arrangement is shown in Fig. 11. The best result was obtained for 55 mA DC current of the laser diode. The gain was 0.58 dB at 2.08 GHz. The measured 3 dB bandwidth was higher than 14%. The calculated and the measured characteristics are sown in Fig. 12. The measurements confirm well the simulated results, however, a shift in the central frequency is observed. The typical spectrum of the received signal is presented in Fig. 13.

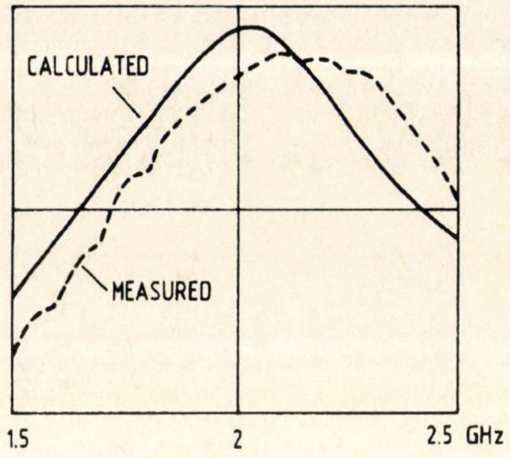

Fig. 12. Link transmission characteristics

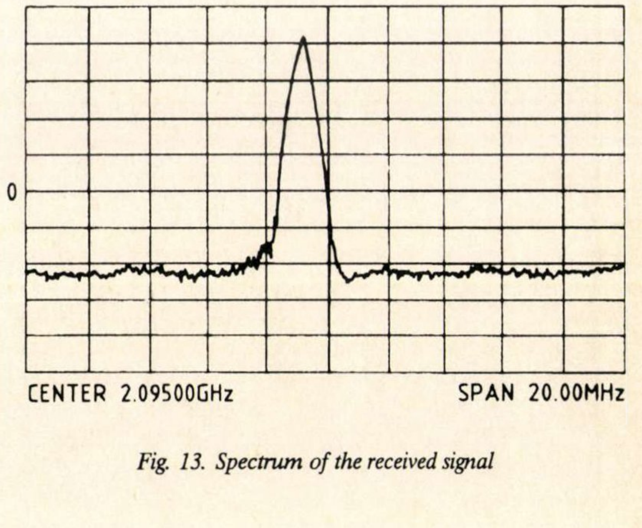

Fig. 13. Spectrum of the received signal

5. CONCLUSION

The microwave matching of optoelectronic devices has been considered. Special attention has been given to laser diodes and photodetectors. Several matching techniques have been reported and applied to the same laser diode. The simulations show that an efficient matching of a chip laser diode could gives a bandwidth higher than 50% for insertion loss of 1.6 dB. Some of the reported techniques has been used to match commercially available Sharp LT022MS laser diode and Mitsubishi APD PD1002 photodetector. These components have been used to realize an optical link for microwave signal. It shows 0.58 dB power gain at 2.08 GHz and a -3 dB bandwidth better than 14%. The experimental results confirm the theoretical predictions. The obtained performance of this optical link shows that an efficient microwave matching of the optoelectronic devices reduce significantly the insertion loss and increases the bandwidth even for optoelectronic devices nonoptimized for high frequency operation.

REFERENCES

[1] Sueta, T., Izutsu, M., "Integrated Optic Devices for Microwave Applications" *IEEE MTT* Vol. 38, no.5, pp.477-482, May 1990
[2] Berceli, T., "New Potentials in Microwave Optoelectronics" 21st *Eu. M.C. Work. Proc.* pp.1-7, Sept 1991
[3] Cox, C. H. III, Betts, G. E., "An Analytic and experimental Comparaison of Direct and External Modulation in Analog Fiber-Optic Links" *IEEE MTT* Vol.38, no.5, pp.501-509, May 1990.
[4] Huff, D. B., Anthes, J. P., "Optoelectronic Isolator for Microwave Application" *IEEE MTT* Vol.38, no.5, pp.571-576, May 1990.
[5] "MDS CAD Package for microwave circuits" *Designer's Task Reference* HP Part Number 85150-90106.

Smail Tedjini received the Matrîse EEA degree from Joseph FOURIER University and the "Doctorat d'Etat Es-Sciences" from INPG (Grenoble, France) in 1980 and 1985, respectively. In 1981 he joined the Laboratoire d'Electromagnetisme Microondes et Optoelectronique (LEMO) in Grenoble. From 1990 he is the head of the Optomicroonde group in the LEMO and his research concerns the optical control of microwave signals and components as well as high speed integrated optoelectronic devices. Dr. Tedjini is a member of IEEE-Microwave Theory and Techniques, SPIE The International Society for Optical Engineering and the French SEE.

Najib El Kamoun obtained his DEA and his Phd degree in microwave engineering and optoelectronics form the Polytechnical National Institute of Grenoble. He has worked in modelling and time domain analysis of interconnection lines for fast logic circuits in GaAs and Si tehcnologies. Since 1990, he has worked on CAD of MMIC's and optical links for microwave signals at the Laboratory of Microwave, Electromagnetism and Optoelectronics, Grenoble.

SI-GE HETEROJUNCTION BIPOLAR TRANSISTORS

P. MÁRTON and I. ZÓLOMI

DEPT. OF ELECTRON DEVICES
TECHNICAL UNIVERSITY OF BUDAPEST
H-1111 GOLDMANN GY. SQUARE 3.

This paper describes a new type of bipolar transistor, where the base is composed of $Si_{1-x}Ge_x$ alloy. As the result of this, the common emitter current gain has been dramatically increased. In the followings we describe how the high current gain can be transferred into high operating speed what recent technics rather requires, and we give some results and examples obtained in the literature.

1. INTRODUCTION

Recently the unity-current-gain cutoff frequency (f_T) in Si-based bipolar transistors, with the help of scaling has already approached or reached that limit, which is determined by the trade-off between the dopant concentration and the width of the base. In consequence of this the most important parameters of the transistors such as current gain, cutoff frequencies, break-down voltages as well as the Early voltage still achieve an optimal values but improving any of them adversely affect the others. One possible way leading out from this loop is the application of heterojunction was first employed with success in that technological area where the realization of this required only little additional expenditure. And that was the area of epitaxial crystal growing where it is relatively easy to build in a third or further materials into the $p-$ or $n-$type lattice of the pn junction. Since this technique has been successfully applied in the compound semiconductors, it was worth enhancing further the operating frequency of this devices by using heterojunctions.

But the active devices made of compound semiconductors for instance GaAs or InP have the certain disadvantages because usually only individual devices are produced, and the GaAs-based microwave monolithic integrated circuits (MMIC-s) haven't achieved the resolution of Si-based ones yet. Partly because of the wafer made of compound semiconductor materials suffers from crystal defects and partly because this technology is not so mature and well-proven as the Si-based one. Therefore an researching activity has been growing aiming at developing the Si-based bipolar transistor as the active element of the Si-based microwave monolithic IC-s or high-speed digital circuits.

2. THE ELECTRICAL PROPERTIES OF HETEROJUNCTION

At a heterojunction the junction is composed of two different kind of semiconductor materials having different band gaps. This two materials can be doped identically or contrary but in case of heterojunction bipolar transistor (HBT) the latter is the essential or in other words the heterojunction is a pn junction as well. In case of Si/SiGe HBTs both the emitter-base and the base-collector junctions are heterojunction since the material of the base is p-type $Si_{1-x}Ge_x$ alloy while the emitter and the collector are made of n-doped silicon. Therefore such devices are often called double HBTs (DHBTs). In the followings we are dealing with only that kind of devices only.

It can be seen from Fig. 1. that the potential barrier blocking the electron diffusion to p-type SiGe has decreased with the value of $\triangle E_c$, and becomes much smaller than the potential barrier for holes, which has an increasing term of $\triangle E_v$, $\triangle E_c$ and $\triangle E_v$ are the conductance and valence band discontinuities expressed in energy while $\triangle E_v + \triangle E_c = \triangle E_g$ makes the whole band gap change.

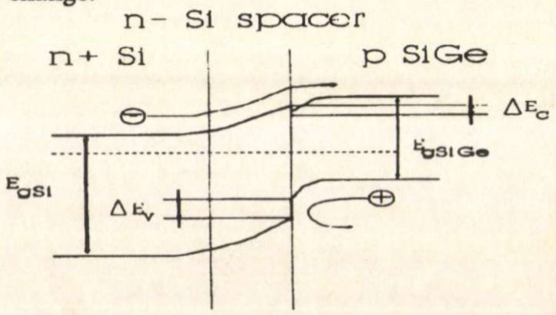

Fig. 1. The band diagram of pn junction applied in HBTs. The breadth of the n-side space-charge layer is increased by the slightly n-doped so called spacer layer.

Therefore the rate of the diffused electron and hole current densities is

$$\frac{j_n}{j_p} = \frac{D_{\mathrm{n(SiGe)}} W_E N_E}{D_{\mathrm{p(Si)}} W_B N_B} \exp(\triangle E_g / kT) \qquad (1)$$

where $D_{\mathrm{n(SiGe)}}$ and $D_{\mathrm{n(Si)}}$ are the electron and hole diffusion coefficients in SiGe and in Si, respectively. W and N denote the width and the dopant concentration of the emitter and base. The exponential factor expresses the enhancement of the electron current density and the decrease of the hole current density. These current densities in the case of a pn homojunction being identically doped as the heterojunction are the followings:

$$\frac{j_{\mathrm{n(hetero)}}}{j_{\mathrm{n(homo)}}} = \frac{D_{\mathrm{n(SiGe)}}}{D_{\mathrm{n(Si)}}} \exp(\triangle E_c / KT) \qquad (2)$$

$$\frac{j_{\mathrm{n(hetero)}}}{j_{\mathrm{n(homo)}}} = \exp(-\triangle E_v / KT) \qquad (3)$$

In practice $2-10$ times enhancement of current density can be observed at room temperature depending on technology and structure [1], [2], [7]. From equation (2) and knowing the temperature dependence of the emitter current the value of $\triangle E_v$ can be derived. This happen to be around $59 \ldots 75$ meV at 12 % Ge as Patton has mentioned [1], [2]. King [4] has determined both the values of $\triangle E_v$ and $\triangle E_c$ and they are proven to be 80 and 50 meV, respectively if the Ge concentration is 10 percent and the base doping concentration N_A is 10^{18} cm^{-3}.

Those valence and conductance band discontinuities may be higher if the base doping has a higher value and the mechanical strain is present in the lattice [8], so the differences of this energy values, which can be found in the literature are easier to explain. The base current densities are even more sensitive to the technology since the decrease of the hole current of the heterojunction could be demolished by the recombination current due to the badly passivated 'mesa' sidewall (see in Fig. 2.), or the interface between Si and SiGe , which are in fact the emitter and base layers. This interface always has more or less recombination centres, which come into being during the technological steps.

3. THE TECHNOLOGY AND STRUCTURE OF HBT

The transistor has a mesa-defined structure as one can see in Fig. 2. After the collector, base and emitter layers are deposited epitaxially by molecular beam epitaxy (MBE) without breaking vacuum, the structure is fabricated using dry etching techniques. Low energy acceptor implantation is used to improve the base contact resistance. Junction sidewall passivation is accomplished using a low temperature deposited oxide. Electron-beam lithography ensures the required small lateral geometry.

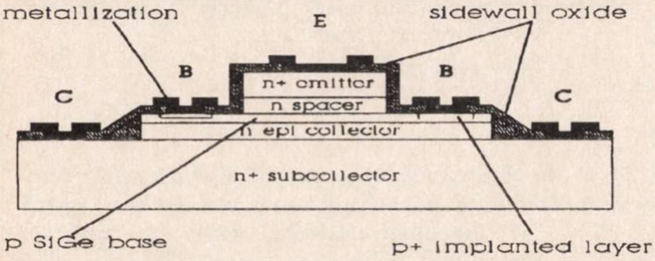

Fig. 2. Typical schematic view of mesa-defined transistor structure. The active emitter area is usually $1 \times 2 \ldots 4\mu m^2$ *[1].*

In the epitaxial process a single-crystalline layer is grown on the single crystal substrate, and the newly grown layer continuities the crystalline structure of the substrate. In case if MBE the components as well as the dopants of the material to be grown are individually evaporated in the special effusion cells, from which the fluxes of the components are directed into the substrate, where the crystal growth is taking place. The temperature of the substrate during the process is $500-600$ °C, and the vacuum is ultra high, notably 10^{-10} mbar. The complete layer sequence of the HBT is grown without braking vacuum including surface preparation and the verification of the qualities of the layers. By this technology a layer containing only a few atomic layer and having any kind of dopant concentration can be done at relatively low temperature, which prevents the diffusion between the two neighbouring layers. Due to the higher level of base dopant concentration the depletion region at the E$-$B junction would be narrower if the so called emitter spacer layer, witch is lightly doped wasn't placed between the base and the emitter. It is done by such a way that the extension of the spacer is hardly more then the extension of the depletion layer. Therefore the depletion region remains fairly wide. Usually the dopant concentration level of spacer are well below the one of the base so nearly all the depletion layer is in the spacer, that is in the emitter. In order to achieve low base-collector capacitance and avoid puncthrough in the base, low doping concentration in the depleted collector is needed, and that serves the n epitaxial layer.

The latest papers have reported their successes in the application of the already existing polysilicon emitter process [2], [3], [7]. This offers a partly self-aligned technology, which has an ability to decrease further the lateral extensions. Beside that a three times base current decrease can also be observed in these devices. In Fig. 3. the simplified schematic cross section is introduced where the SiGe base layer was deposited on substrates patterned by recessed oxide (ROX) isolation. The shallow n^+ poly emitter contact was formed using furnace and rapid thermal annealing (RTA). But this polysilicon process also has a drawback notably the increased emitter serial resistance $r_{ee'}$.

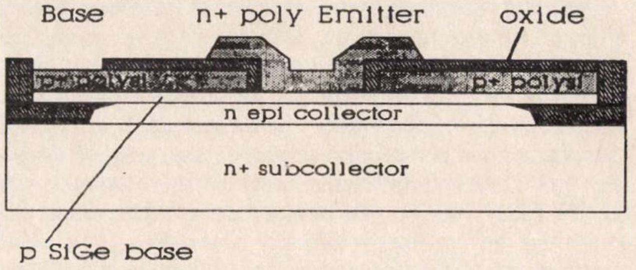

Fig. 3. Simplified schematic view of the HBT having polysilicon emitter contact. The base is also contacted by polysilicon due to the poly-emitter bipolar process [3].

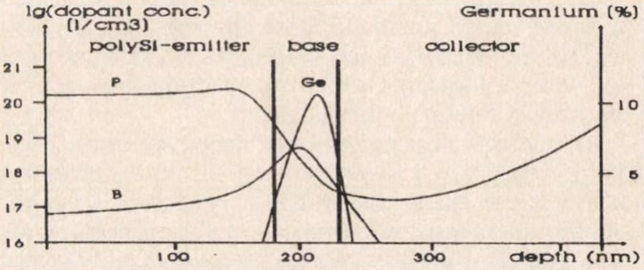

Fig. 4. Impurity profiles obtained by secondary ion mass spectroscopy (SIMS) in polysilicon contacted HBTs.

4. THE POSSIBILITIES GIVEN BY THE HETEROJUNCTION

The cutoff frequency (f_T) of a bipolar transistor is determined by the following terms:

$$\tau_{\mathrm{ec}} = \frac{1}{2\pi f_T} = r_{\mathrm{cc'}} C_{\mathrm{bc}} + r_e C_{\mathrm{eb}} + \frac{S_{\mathrm{bc}}}{2v_{\mathrm{th}}} + \frac{W_b^2}{D_{\mathrm{nb}}} F_{(N_B)} \tag{4}$$

where

$$r_e = r_d + r_{\mathrm{ee'}};\ r_d = \frac{U_T}{I_E}; \tag{5}$$

- U_T is the thermionic voltage, I_E is the d.c. emitter current, and $r_{\mathrm{ee'}}$ is the serial emitter resistance,
- $r_{\mathrm{cc'}}$is the collector serial resistance,
- C_{eb} and C_{bc} are the E$-$B and B$-$C space-charge capacitances,

- S_{bc} and W_b are the widths of the B – C depletion layer and the neutral base,
- v_{th} is the thermal velocity of electrons in the B – C depletion region,
- D_{nb} is the diffusion length of electrons in base,
- $F_{(N_B)}$ is the base-profile factor of the base.

If the serial base resistance $r_{bb'}$ happen to be significant, the maximum oscillation frequency can be smaller than the unity current gain frequency:

$$f_{max} = \left(\frac{f_\alpha}{8\pi r_{bb'} C_{bc}}\right)^{\frac{1}{2}} \tag{6}$$

Let's examine that how and why the individual time constants of (4) are altered at HBTs. The direct effects of E – B heterojunction is in reducing the base current density if the emitter current is supposed to be the same as in the case of homojunction. This appears in decreasing the storage time of the emitter. But this term hasn't got a significant role in the homojunction bipolar transistors, not even in HBTs. In contrast with the direct effects the indirect has the main essence. Since usually there is no need to create a transistor having ultra high common-emitter current gain but we require all the more the one having high cutoff frequency, therefore the possibility presents itself to increase the base doping density (N_B), and make the base layer thinner, while the Early voltage still remains reasonable, because due to the stronger base doping the space-charge region doesn't extend into the base so deeply, and the base doesn't becomes thinner. The so called base profile factor $F_{(N_B)}$, which is eventually describes the built-in electric field in the neutral base becomes smaller due not only the gradient of base dopant but to the gradient of the Ge percentage as well (graded-SiGe-base) [2], [3], [7]. While the born concentration decreases towards the collector the Ge fraction shows the opposite tendency generating further 30 – 40 kV/cm electric field (Fig. 4.). Finally the decrease of $F_{(N_B)}$ makes the forth term of the left hand side of equation (4) smaller, but this term, which is the base transit time, is going to be even smaller since the width of base also reduced. The second term of (4) has also become smaller because r_e, the emitter serial resistance is reduced due to the thinner emitter layer, and C_{eb}, the E – B space-charge capacitance is also reduced due to the emitter space, which makes the space-charge layer wider. The first term in (4) more or less remains the same because the n^+ subcollector is doped as high as possible, the n-epi collector is as thin as it has to be to include only the spacer-charge region of the reverse biased B – C junction and therefore $r_{cc'}$ doesn't change in consequence of applying heterojunction. The main difference compared to the common silicon transistor is that the E – B space-charge layer is mainly in the material of emitter (notably in the emitter spacer layer) and not in the base. The width of the B – C depletion layer (S_{bc}) can be adjusted by varying the n epitaxial collector concentration. The increase of the B – C depletion layer although decreases the B – C capacitance, but increase the third term of (4). The symmetry of the emitter and the collector doping concentration appears in the inverse common emitter current gain, being more than 50 percent of the normal gain, even though the area of the inverse emitter-base junction is about five times larger that of the normal emitter-base junction [5]. In order to reach a high maximum oscillation frequency, f_{max} the $r_{bb'}$ base serial resistance also should be reduced as the (6) equation it shows. The dominant part of $r_{bb'}$ is due to the active intrinsic base, which is disadvantageously affected by reducing its width since the base current flows in lateral direction.

5. THE OPTIMAL GE FRACTION

Determining the optimal Ge fraction needs optimization considering several influencing effects having beneficial or disadvantageous effect on the transistor performance. One of these is the reduced electron mobility in the SiGe base caused by additional alloy scattering. In the literature this taken into account by the way that the electron mobility in p-type silicon $\mu_{n'}$ is combined with the alloy-scattering-mobility of $Si_{1-x}Ge_x$ alloy μ_A by using "Matthiessen's rule" [10].

$$\mu_n\big|_{SiGe} = \mu_n\big|_{Si} \times \mu_A\big|_{SiGe} \tag{7}$$

$$\mu_A\big|_{SiGe} = \frac{9.7 * 10^3 * T^{-0.8}}{x(1-x)} \tag{8}$$

where T is temperature in K, x is Ge fraction under the condition of $0 \leq x \leq 0.8$. The value of μ_A comes from (8) is in cm^2/Vs. So from this point of view the Ge content has a certain drawback.

The main reason why the Ge has been applied is to decrease the band gap in the base and therefore the more Ge the base contains the better can prevail its beneficial influence.

We have to take this question into consideration from technological point of view as well. The lattice constant of the germanium is bigger than the one of silicon by 4 % and therefore the SiGe layer deposited in silicon has biaxal compressive mechanical stress. It is also crucial that the coefficient of thermal expansion of the two materials be close to each other. If they do not, or in other words the Ge percentage is high enough, this effect can cause technological and indirectly electrical problems. It has to be mentioned that the mechanical stress being either tensile or compressive lowers the band gap of the strained layer [8]. It is worth increasing the Ge content in the base only till that limit, where the beneficial effect of Ge is entirely compensated by the disadvantageous effects, in respect of a chosen parameter. This parameter is usually the F_T cutoff frequency which is mainly increased by the decrease of the last term on the left hand side of equation (4), as it has been mentioned already. After a certain Ge percentage this term become smaller than the other three altogether, and the higher germanium content only serves to decrease the electron mobility in the base. The electron mobility being about three times larger at low temperature than at room temperature as well as the higher current gain make the cutoff frequency higher at 77 K. Finally the f_T cutoff frequency reach its maximum in a range of $x = 0.1 \ldots 0.3$ and beyond it f_T begins to decrease slightly [10].

6. RESULTS AND EXAMPLES

The transistor optimization is carried cut by fulfilling the following requirements:

- f_{max} shold be equal or higher than f_T at high current densities,
- f_T and f_{max} should be as high as possible,
- these frequencies shold also be high at low current densities,
- beside that, the transistor should have fairly high current gain.

Table 1.
Various profiles obtained and their expected theoretical properties.

Parameter	Si/SiGe	Si/SiGe	GaAs/GaAlAs	Si/Si	Si/Si
Base width [nm]	20	20	34+60	20	20
dopant c. [1/cm^3]	4.6 E18	5.5 E18	3−0.02 E19	5.0 E18	1.0 E19
n-epi collector width [nm]	200	200	80	200	200
dopant c. [1/cm^3]	1.5 E17	2.3 E17	4−10 E17	2.4 E17	4.0 E17
Emitter spacer width [nm]	50	50	40	–	–
dopant c. [1/cm^3]	5.1 E18	2.0 E19	2.0 E17	–	–
Emitter width [nm]	–	–	40	50	50
dopant c. [1/cm^3]	–	–	1.0 E18	1.0 E19	4.0 E18
Temperature [K°]	77	300	300	77	300
Ge or Al [%]	20	20	30	0	0
f_T [GHz]	300	106	242	240	–
f_{max} [GHz]	325	118	284	273	125
β	6 E3	15700	–	6.1	0.79

While the dependence of current gain on current density in HBTs is the same as in the Si/Si structure, the dependence on the temperature is quite different. The reason is to be found in equation (1) where the smaller temperature enhances the effect of band gap narrowing. For example the increase of the collector current is found to be 5.7 times at 300 K and 1000 times at 90 K [1]. Therefore it is necessary to make special designs at different temperatures. A transistor optimized for 77 K is not a good one when it is used at room temperature. By lowering a temperature from 300 K downto 77 K, the maximum frequencies can be increased by the factor of two. Table 1. summarizes the various designs and their theoretical properties [9]. The Si/Si bipolar transistor also shows good high-frequency properties at 77 K and 300 K, but because of a very low β-value it is out of any interest. Considering the four requirements mentioned in this chapter, the most beneficial transistor has been reported in [6]. This device exhibits 500 V Early voltage, a maximum room-temperature current gain of 550, and an f_{max} of 40 GHz while the f_T transit frequency reaches 42 GHz.

7. CONCLUSIONS

The $Si/Si_{1-x}Ge_x$ DHBT has excellent current gain and good frequency characteristics at 300 K and even at 77 K and can therefore be widely used in applications where the ordinary silicon bipolar transistors have not enough good. In combination with the emitter and the collector interchangeability, and the possibility to use semiinsulating silicon substrates in $Si/Si_{1-x}Ge_x$ DHBTs is very useful when designing millimetre wave or high speed digital circuits with silicon technology.

REFERENCES

[1] Patton, G. L., "Silicon-Germanium-Base Heterojunction Bipolar transistors By Molecular Beam Epitaxy" *IEEE Electron Devices Letters*, vol.9, No.4, pp.165-167, 1988.

[2] Patton, G. L, "Graded-SiGe-Base, Poly-Emitter Heterojunction Bipolar Transistors" *IEEE Electron Devices Letters*, vol.10, No.12, pp.534-536, 1989.

[3] Patton, G. L., "75-GHz SiGE-Base Heterojunction Bipolar Transistor" *IEEE Electron Devices Letters*, vol.11, No.4, pp.171-173, 1990.

[4] King, C. A., "Si/SiGe Heterojunction Bipolar Transistors Produced by Limited Reaction Processing" *IEEE Electron Devices Letters*, vol.10, No.2, pp.52-54, 1989.

[5] Kamis, T. I., "Small-Geometry, High-Performances, $Si - Si_{1-x}Ge_x$ Heterojunction Bipolar Transistors" *IEEE Electron Devices Letters*, vol.10, No.11, pp.503-505, 1989.

[6] Gruhle, A., "MBE-Grown Si/SIGe HBT's with High β, f_T, and f_{max}" *IEEE Electron Devices Letters*, vol.13, No.4, pp.206-208, 1992.

[7] Crabbé, E. F., "73 GHz Self-aligned SiGe-Base Bipolar Transistors With Phosporus-Doped Plysilicon Emitters" *IEEE Electron Devices Letters*, vo.13, No.5, pp.259-261, 1992.

[8] Jain, S. C., "The combined Effects of strain and Heavy Doping on the Indirect Band Gap of Si and SiGe Alloys" *Solid-State Electronics*, vol.34, No.5, pp.445-451, 1991.

[9] Karlsteen, M., "Optimized Frequency Characteristics of Si/SiGe Heterojunction and Conventional Bipolar Transistors" *Solid-State Electronics*, vol.33, No.2, pp.199-204, 1990.

[10] McGregor, J. M., "On the Optimum Ge Fraction in Si/SiGe Heterojunction Bipolar Transistors" *Solid-State Electronics*, vol.34, No.9, pp.1019-1021, 1991.

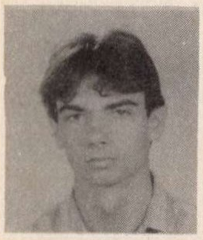

Péter Márton received his M.S. degree in 1991 from the Technical University of Budapest, Faculty of Electrical Engineering, in Microelectronics. Since September of 1991, he has been working for his Ph.D. degree at the Department of Electron Devices, TU. of Budapest. His interests include microelectronic technology as well as modelling and studying of new electronic devices. He succesfully took part in the Senior Student Conference in 1991. He is a Student Member of IEEE.

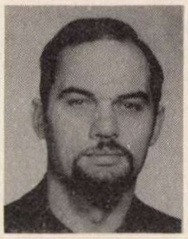

Imre Zólomy graduated in electrical engineering at the Technical University of Budapest in 1965. Since then he has been with the Technical University of Budapest, at the Department of Electronic Devices. he received his "dr. tech." degree in 1974, and the Candidate of Technical Sciences Degree in 1983. At present he is a Reader in Technical Sciences. He is the chairman in the Committe of Foreign Affairs of the of the Scientific Society for Telecommunications, and the Secretary Semiconductors and Integrated Circuits Section. His research area is the Physics of semiconductor devices, mainly the study and modelling at devices having extra-small size or novel operating principle, such as tunnel-oxide devices and polysilicon emitter transistors.

ESSDERC'92

The 22nd European Solid State Device Research Conference was organized this year in Leuven (Belgium). It was focused on the physics, characterization, processing and application of solid state devices. 450 scientists from 28 different countries participated in ESSDERC'92. The conference programme featured 33 invited and 162 contributed papers and a Panel Discussion on *The impact of new technologies on future systems*.

The conference papers and the Panel Discussion emphasized, that the ultra low power requirement will be the major driving force in the next decade, achieved by the utilization of very expensive production lines capable for submicron CMOS ($\leq 0.5\mu$m) BiCMOS circuits may also play a major role due to their higher speed, low powerline noise and easier design.

With the scaling down of CMOS design rules to 0.25μm, circuit performance improvement can be achieved. New design ideas, such as memory-logic cointegration, GaAs–Si CMOS integration, ferroelectric thin films for non-volatile memories (FEARAM), hybrid optoelectronics (InP–ECL or CMOS circuit cointegration), integrated optics etc. offer a route to overcome the limitations of former IC's.

The new construction goals of consumer electronics are hand-held digital devices. Such a new device, called ICARUS has been outlined at Phillips Research, providing a large number of functions either directly or by remote access to central resources and services through a cellular communication network. These services may be the following: watch (local), audio/video (local mini CD), telephone (cellular), data-retrival (network access to data banks), electronic credit card and/or personal id-card (passport), travellers route guider (with its local mini CD and with some remote functions), translation from/to foreign languages with speech output (by access to a translate server), remote control of different household apparatus (eg. heating), etc.

ICARUS should have an LCD, a mini CD drive, audio I/O including human speech, and a limited amount of integrated electronics combined with a UHF radio link which provide access to central data and computing resources over a cellular telephone network. This design concept poses major challenges to IC technology:

- high frequency (GHz) technology for frontends (eg. Si–Ge devices),
- low power, low voltage CMOS technology for analog and digital functions,
- some non volatile functions (credit card, passport),
- very compact packaging (eg. multichips modules).

For the communication industry (representing about 7% of the world IC market) the most important feature is the transistor density on the chip. Therefore a shrinkage of the transistor gate length from $0.7 - 0.8\mu$m (1992) down to $0.5-0.6\mu$m (expected in 1996-97) and further down to 0.35μm accompanied by the increase of the chip size, the decrease of the power supply voltage (changing the 5 V standard for 3.3 V in almost every application) and the application of multilevel metalization is needed.

The key process technologies for transmission systems (speed $\leq$ 2.4 Gbit $\cdot\, s^{-1}$) are HF-bipolar (either poli-Si emitter or Si-Ge devices and CMOS.

There are indications, that *photonics* bulk effect solid state devices) may mature in the beginning of the next century and will take over many electronic functions. Some early examples for such devices are the optical amplifiers, optical switches and various quantum-well devices.

The new concepts impose many problems for process and device engineers. The design of the state-of-the-art device structures requires accurate, robust, and user-friendly CAD tools.

Devices based on quantum-mechanical effects need simulation tools capable of dealing with such problems. Heat conduction may also play a major role during the operation of many devices (eg. in casc of SOI circuits), thus the simulation of the carrier heating and the energy balance equations became crucial in present device simulators.

The design of sub-μ or even deep sub-μ processes requires lots of trade-offs between technological possibilities and the electrical performance of the fabricated devices. This field has been recently classified as *manufacturing science*. For making the right decisions during process development the integration of process and device simulation is of great importance. This is a way, how technology CAD systems (T-CAD) play a major role in progress of the IC technology.

Summarizing the statements of the conference, it is obvious, that

- besides computer industry, telecommunication and consumer electronics in the next two decades will have their own input on technology with their special demands as driving force. There will be no device structure changes down to 0.25μm minimal feature size in the workhorse, SI-based CMOS technology, but there will be changes in process design to satisfy the higher performance demands.
- to achieve complex logic circuitry and high packaging density in new telecom systems, optical devices and VLSI-CMOS circuits have to be integrated on the same silicon chip. Fast laser diodes integrated with transistor drivers on an intermetallic substrate (InP) will help to lower the cost of fiber optic communication devices.
- to reduce circuit complexity in certain analog and digital applications quantum devices (eg. resonant tunneling bipolar transistors – RTBTs) may be applied in the mext 10–20 years (FUJITSU Laboratories, AT&T).

A. POPPE
Dept. Electronic Devices
TUB

TEKTRONIX TFP2 FIBERMASTER – OPTICAL TIME DOMAIN REFLECTOMETER

Equipped to accommodate two dual-wavelength optical plug-in modules at the same time, the FiberMaster^{TM} allows users the flexibility of high-resolution and long-range performance in singlemode and multimode applications, all in the same instrument and at the touch of a button.

The high-resolution color FiberMaster^{TM} sets a new level of performance and flexibility, providing faster, easier, more efficient solutions to fiber optic testing requirements.

FiberMaster is the only OTDR equipped to accommodate two dual-wave-length optical plug-in modules at the same time. Fully utilized, this features gives the user dual-wavelength singlemode optical cable testing at a touch of a button. In addition, each plug-in module combines high-resolution and long-range performance. This allows testing of virtually any communications network (Telco, cable TV or LAN) without switching modules.

FiberMaster is driven by advanced Motorola 68020 technology, giving the user a high-speed, 32-bit processor that delivers clear, concise accurate waveforms in a fraction of the averaging time taken by other OTDR systems which are based on traditional PC technology.

FiberMaster sets a new testing standard with its unique of exclusive features. An expandable overview/window design lets you switch from the big picture to details and back again easily and quickly. Window set-up menus are user friendly with automatic help screens triggered by context sensitive single function front panel controls. Soft keys, high resolution full-color graphics, high resolution, high speed internal printer and a broad selection of mass storage options combine to make the FiberMaster the most comprehensive, easiest-to-use optical time domain reflectometer available

KEY FEATURES, BENEFITS

High Speed Processing System

FiberMaster is driven by a high-speed 32-bit processing system. This result in clear concise waveforms in a fraction of averaging time executed by traditional OTDR systems.

Extremely Easy to Use Human Interface

By offering overview/windowing design, soft keys,single function front panel controls, window setup menus, and context sensitive help, the FIberMaster is very easy to use. Minimizing training time for first time users and recall time for occasional users results in increased productivity.

State of the Art Color Display

FiberMaster is the first high performance OTDR with high resolution color. Color provides a more dynamic display and is especially useful when making multiple waveform comparisons and differentiating events on the waveform. The dynamics of color aid in the reduction of user errors. A monochrome version is also available.

High Resolution CRT Display

Not only is the FiberMaster's display available in color, it is the highest resolution OTDR display available, with 640 × 480 pixels on a 7 inch diagonal screen. This results in enhanced understanding and analysis of waveforms. Users will be able to see fiber better then they have ever been able to see it before.

Dual Optical Plug-in Capacity Mainframe

Fibermaster is the only OTDR equipped to accommodate up to 2 separate optical plug-in modules at the same time. This feature gives the user dual wavelength multimode and dual wavelength singlemode optics at the push of a button. This allows testing of practically any communications application without having to manually switch modules.

Custom Configurable Design

The customer has the flexibility of ordering FiberMaster equipped with as much, or as little as he wants, depending upon his testing requirements and budget. Custom configuration is done simply by specifying options as desired. Field interchangeable optics plug-in modules are selectable by option when ordering the instrument, or can be ordered separately and installed in the field at the user's convenience.

High Resolution Internal Printer

Hardcopy documentation of the waveform and support data can be obtained in less than 15 seconds. The resolution is the same as the CRT display (150 dots per inch) which provides the user with a permanent record of equal clarity as the high resolution screen.

Mass Storage

A selection of factory installed mass storage devices are available when ordering FiberMaster to provide multiple waveform storage and recall. FiberMaster is fully MS/DOS file compatible which allows interaction with PC systems. The customer can select from a 3.5 inch floppy disk drive, suitable for most commercial applications, or a removable RAM card drive system for ruggedized environments, and/or 1 Mbyte internal RAM storage capacity.

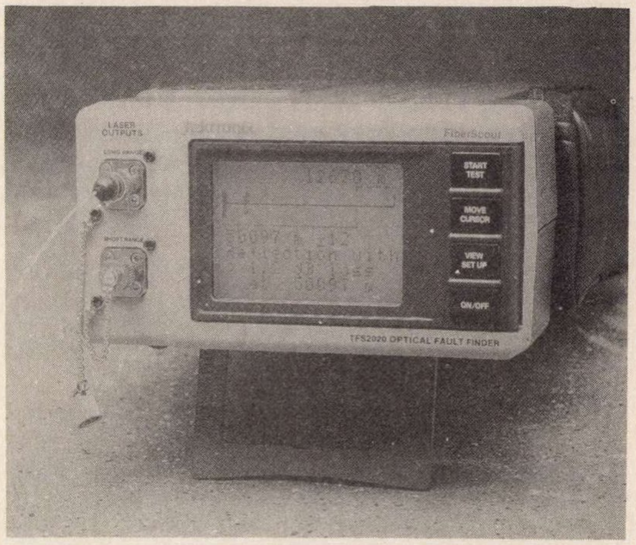

For further Information please contact Tektronix Rep. Office Hungary, Horvát u. 2–12. IV. em. 39., 1027 Budapest, Phone: 36(1) 201 6442

OPTICAL CABLES BY PIRELLI

PIRELLI CAPABILITIES

Pirelli is one of the largest international producers of cable with annual sales in excess of US 4 Billion. The group has cable factories in 10 countries and covers the spectrum of international requirements ranging from state of the art Optical Fibre and Cable to Super Tension Energy Cables. Pirelli produces Optical Fibre using each of the three major technologies, namely OVD, VAD and MCCVD, and is the largest producer of singlemode Optical Fibre in Europe.

In the UK, Pirelli Communication Cables Division is the market leader by volume of Optical Fibre Cables and has been producing these cables since the late 1970's.

The Division's business/operating philosophy is based upon a Total Quality Management (TQM) approach and all products and services are subject to a continuous improvement process. The philosophy is underpinned by comprehensive training for all employees and an operating culture that encourages and recognises the contribution of all employees in the success of the business.

Few companies have the international pedigree and repulation for quality as Pirelli Communication Cables Division. In the UK, they are the largest manufacturer of optical fibre cables, while their parent, Pirelli, is one of the dominant cable groups in the world.

In addition to Pirelli's ability to provide turnkey solutions for underground cable applications, they have extensive expertise and experience in the field of aerial cables. Pirelli has been installing aerial cables for over a century and nowadays excels in the area of self-supporting fibre optic cables,

Before entering into a contract Pirelli will analyze all the technical information to ensure that customers receive the correct cable specification for their requirements. On some occasions the route will be surveyed, and where necessary a theodolite linked to a computer utilised to collect accurate information about the supporting structures and surrounding topography.

The Division is BT's (British Telecom) number one supplier of communication cables, and provides Germany's Deutsche Bundespost Telekom with Optical Fibre Cable.

Hundreds of kilometers of Pirelli cables were successfully installed by many Hungarian companies.

In the followings the products currently being supplied to the Hungarian market are outlined. Pirelli will be pleased to provide quotations for these products and to recommend designs for other Optical Cable applications within Hungary.

OPTICAL TRUNK CABLES

Underground Cables and Duct Cables

Pirelli can provide a wide range of metallic or nonmetallic duct cables. The majority of cable types are suited to CaTV applications. The cables currently being provided are non-metallic and contain 6, 10, 20, 30 or 40 fibres. The fibres are individually coloured for easy identification and a cross-sectional diagram of a typical duct cable is shown in Figure 1.

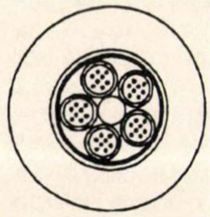

Figure 1. Multi element duct cable

The construction involves five loose tubes stranded around a central strength member. The loose tubes each contain up to eight singlemode optical fibres. The spaces between the tubes and also the tube interior are filled with a water blocking compound in the event of the cable becoming damaged after installation. Polyester tapes are used to firmly bind the cable, and a protective layer of Aramid yarns are applied over the tapes to provide additional tensile strength. Finally, a polyethylene jacket is applied to the cable. The jacket is overprinted with customer and product information to ease identification.

Directly Buried Cables

Additional protective layers of corrugated steel tape and polyethylene can be added to the basic duct cable construction to provide cables suitable for direct burial.

AERIAL CABLES

Short Span Installation

This family of cables is designed for installation from wooden, steel or concrete poles which are located up to 80 metres apart. The cables can be of all dielectric (non metallic) construction or may contain metallic elements if required for a particular application. In addition, the cables can be circular self supporting, circular but lashed to an independent strength member, or of figure-of-eight construction. An example of a cost effective self supporting cable is shown in Fig. 2b. This type of cable is particularly applicable for rural applications and the cable can also be installed in underground cable ducts.

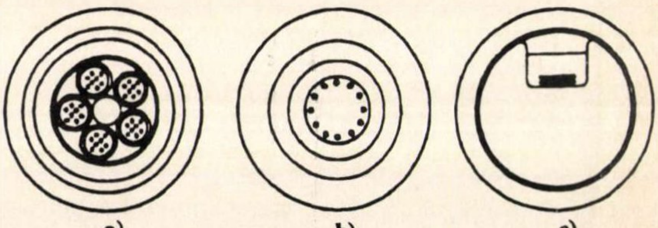

a) b) c)

Figure 2. Aerial cables.
a) Aerial multi element; b) Aerial ruggedised loose tube; c) Fibrespan

Long Span Self Supporting Optical Fibre Cables

Pirelli manufactures Fibrespan; a high performance, all dielectric, self supporting cable for long span applications up to 1 km (see Figure 3.). The cable can contain up to 24 singlemode fibres and is usually suspended from existing high voltage electricity towers and is located independently of the power (phase) conductors and ground wire. Typically the cable is fixed at the centre of each suspension tower, and on the leg of heavy-angle towers. Fibrespan can be installed during live line conditions. Pirelli is able to offer all accessories necessary to erect the cables and can provide a comprehensive training and installation service.

INTERNAL CABLES

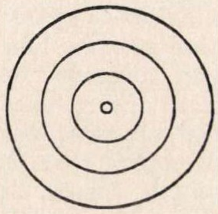

Figure 3. Internal single fibre cable (SFC)

Duct type cable can be offered with an LSOH material (instead of a polyethylene) jacket, which can offer superior fire safety performance. This type of construction is particularly appropriate for in-building installations.

DIGITAL AND PATCHCORDS

A variety of connector styles can be assembled onto the Pirelli SFC (single fibre cables) to create optical patchcords which interface with transmission equipment of any manufacture.

Pigtails and patchcords are available in a range of standard lengths, or can be specially manufactured to customer requirements.

OPTICAL DISTRIBUTION RACKS

Pirelli can supply slimline Optical Distribution Racks for Trunk Backbone Networks.

These units represent an outstanding solution to the conflicting requirements of minimum space utilisation and avoidance of bending losses in the singlemode fibre. For buildings where vertical space is restricted, a variety of options can be offered, ranging from rackmounted termination shelves, to wall-mounted racks or boxes with flying pigtails or patchcord connections.

OPTICAL CABLE CLOSURES AND SPLICING ACCESSORIES

Pirelli can supply joint closures for all types of cables, both underground and aerial. They can accommodate both straight or spur joint in either a straight-through or dome-ended configuration. Special requirements, such as shotgun protection for above ground joints or additional physical protection for buried joints, are accommodated within range of available products. All items come with the added security of approval by Pirelli's engineers for the specific application for witch they are supplied.

SPLICING AND TEST EQUIPMENT

Pirelli's installation expertise is always available for the assistance of our customers. Our experience, in many different environments, gives us a good understanding of which equipment is appropriate for field splicing and testing of optical cables. Depending upon the customer's requirements Pirelli can advise and recommend for direct purchase or supply and provide after-sales support.

SERVICES

Pirelli can also provide engineering, installation and project management services to assist customer implementation programmes.

Further information:
Pirelli Cables Limited
Hungarian Representative
Minerva u. 2.
H-1118 Budapest
Phone/Fax: 185-2597

EUROPA TELECOM'92 IN BUDAPEST

The Telecom Forum and Exhibition held in every four years in Geneva has been always a special occasion for the telecom world. Lectures showed the latest usable results which were supported by exhibited samples of equipment or by beautifully designed products to be introduced soon in the market. With the aim to make this important event available for distant countries, from the mid-eghties Telecoms were also held in Asia, Africa and Latin-America showing development directions for the next years to experts of these territories.

In Europe Telecom was not organized until 1992, bearing in mind that the global Telecom in Geneva is available to all experts in Europe. However, changes in CEE (Central and East European) countries persuaded the leaders of the International Telecommunications Union to organize a forum and an exhibition in this region as well. The organizational right of the first Europa Telecom'92 was given to Hungary. Notwithstanding, the economic control and the professional program organization was handled by the ITU itself, having a decade-long routine in this kind of matters.

The Forum comprised Policy, Technical and Economic Symposia. The significance of the Policy Symposium was raised by the presence of high ranking state leaders. Among lecturers there were a number of ministers, chairmen of international bodies, executive directors and chairmen of boards of multinational companies present. The views of the high-ranking lecturers were especially important because these people have the power to implement their concepts. It seemed, that their main objective is to create a competitive environment, in the near future. A prerequisite for this is a well organized standardization.

At the Symposium the importance of telecommunications was underlined, interrelations with the development of the society as well as the questions relating to market organization were emphasized. However, in these fields nothing new was heard by the audience. Anyway, it was good to hear that all principles, which were underlined several times by experts in the past two years, were repeated by leaders being in control position.

Among lectures at the Policy Symposium some dealt with the role of user groups and their relationship to telecom services providing some new elements for us. Leaders from Italy, Sweden, Norway and the UK had the unanimous view that these groups help telecom services with their opinions and their constructive criticism. Their consultations promote determination of development directions and on the basis of user's opinions investors can hope with a greater possibility that the sums invested in quality and quantity developments will soon be returned.

Mobile telecommunication was a special topic at the Symposium. In relation to that it is necessary to mention, that at the Policy Symposium there was also a mobile section. The advantages of radio interconnection was also mentioned in rapid developments, the implementation of their real mobility through all Europe, and finally in those methods which lead us from the present mobile systems to the personal telecommunications of the next decade. I must mention that from the approx. 15 lectures dealing with mobile questions, only one or two introduced new solutions or methods, the others mainly dealt with their importance and future. The importance of the new European System, GSM was emphasized while its operational usage has started this year.

Most new ideas were elaborated for the better usage of networks. Along with this, introduction of network intelligence, its application for the purpose of Virtual Private Networks, the practical use of Network Management in increasing traffic forwarding ability, were the subjects which will be possibly used in the Hungarian telecommunications within a short time.

In connection with broadcasting, the importance of digital audio broadcasting (DAB) and higher definition television usage (HDTV) were stressed. During discussions it cropped up, that these new systems can only spread quickly, if they are at least partially compatible with the existing equipment. These kind of solutions have not been mentioned yet by any of the developing companies. This is why a lot of people think that the several billion pieces of equipment, being now in the possession of the population represent a value, which would limit the introduction of these new facilities. The manufacturers have a different opinion, however, they say that in the voice services CD quality and in video technology sharpness and colour resolution common in the movie screens would be a demand for everyone sooner of later; if not, they would try to achieve this situation with the necessary publicity.

In connection with the Technical Symposium it has to be mentioned that notwithstanding the valuable presentations, that with only a year after Geneva a regional symposium can hardly bring anything new. This is especially valid because for the Geneva Symposium the 150 – 200 lectures were chosen from several thousands, with the aim to find those containing some new ideas. Here invited lecturers were reading their texts and the invitations were made upon the fact that they were known to be experts in their own fields. These criticisms were mentioned by leaders and organizers of the ITU being present here.

Most new ideas were introduced at the Economic Symposium. Here some general subjects were also mentioned like economic growth and its relationship with telecommunications, as well as questions related to privatisations and competition, at the same time subjects, which were rarely discussed earlier, came out like tariff politics, leasing fees in cases, when wide competition can not be ensured, monopolies still exist, and the parliament do not prescribe any more telecommunications tariffs. It was also interesting to hear questions arising over the coverage of investments, its speed of return, and the analyses of the question, what kind of services are to be introduced to achieve return of the invested sum. Of course introduction of mobile services has a high rank among services to be introduced.

Following the one or two general lectures in all these subjects in some cases a history of the situation of countries and their views were also in the programme. It was especially interesting to hear the experiences from countries with state-of-the-art telecommunications infrastructure and of the first steps being taken to privatisation, for the creation of a solid competition situation and in the field of creating economic methods in the CEE countries.

It seemed according to the above mentioned that the most progressive changes occurred in the economical platform in the past few years and that is why lecturers in the economic section could bring along new ideas to that of in Geneva. It is also true, that economic presentations for a given region can be more specific than technical results. With the above in mind we can recommend to everyone to read the published volume of Economic Symposium of Europa Telecom.

At the exhibition held simultaneously with the forum mobile telecommunications played also an important role. GSM had place and role, besides CT2 providing limited mobility, and in the pavilion of Motorola we were introduced to its future variation, and with the state of development of personal telecommunications system called iridium which will be implemented by help of satellites at an orbit near the earth. When no problem would occur to send the satellites to their orbits, then in the years of 1996–97 the operation of the technology got a great share, too. At the exhibition several exhibitors introduced construction, installation and measurement facilities to be used implementation of optical cable networks.

In other pavilions we could introduce ourselves with practical applications of new services and facilities. ITU placed the exhibitors price on a very high level, so some of them had to build smaller pavilions. This caused a feeling of underrepresentation in some of the cases like Bundespost Telecom. AT&T also used only a small place compared to its ranking. The exhibition would have deserved more visitors, as young engineers and telecommunications technical and economical experts could introduce themselves with the technology of the following years.

At the exhibition the pavilion of HTC Ltd was remarkable. It was visited by a number of people for its tasteful formation, its rich professional content and the polite handling of the visitors. It was a good propaganda for HTC. Beside HTC, WESTEL and Hungarocom tried to create a favourable image of themselves. Other domestic exhibitors also present, we can say that the Hungarian telecommunications played a leading role at this exhibition.

Summarizing the above, we can say that the presentation of EUROPA TELECOM'92 brought new ideas in some of the technical fields, the whole exhibition was a spectacular event, and it was a good propaganda for the whole Hungarian telecommunications. If some more visitors came, more beautiful remembrance could be left.

GY. LAJTHA
HTC Ltd.

Information for authors

JOURNAL ON COMMUNICATIONS is published monthly, alternately in English and Hungarian. In each issue a significant topic is covered by selected comprehensive papers.

Other contributions may be included in the following sections:

- INDIVIDUAL PAPERS for contributions outside the focus of the issue,
- PRODUCTS-SERVICES for papers on manufactured devices, equipments and software products,
- BUSINESS-RESEARCH-EDUCATION for contributions dealing with economic relations, research and development trends and engineering education,
- NEWS-EVENTS for reports on events related to electronics and communications,
- VIEWS-OPINIONS for comments expressed by readers of the journal.

Manuscripts should be submitted in two copies to the Editor in chief (see inside front cover). Papers should have a length of up to 30 double-spaced typewritten pages (counting each figure as one page). Each paper must include a 100–200 word abstract at the head of the manuscript. Papers should be accompanied by brief biographies and clear, glossy photographs of the authors.

Contributions for the PRODUCTS-SERVICES and BUSINESS-RESEARCH-EDUCATION sections should be limited to 16 double-spaced typewritten pages.

Original illustrations should be submitted along the manuscript. All line drawings should be prepared on a white background in black ink. Lettering on drawings should be large enough to be readily legible when the drawing is reduced to one- or two-column width. On figures capital lettering should be used. Photographs should be used sparingly. All photographs must be glossy prints. Figure captions should be typed on a separate sheet.

For contributions in the PRODUCTS-SERVICES section, a USD 110 page charge will be requested from the author's company or insitution.

JOURNAL ON COMMUNICATIONS IN 1993

In the coming year 1993 we are continuing our practice to publish English and Hungarian issues of this journal. English issues will be devoted to topics in which Hungarian activities may be of international interest, Hungarian issues will be surveying important topics of telecommunications related to our domestic developments.

The topics of the planned issues are the followings:

ENGLISH ISSUES:

- PERSONAL COMMUNICATIONS
- NEURAL NETWORKS
- SEMICONDUCTOR MODELLING
- TELECOMMUNICATION MEASUREMENTS

HUNGARIAN ISSUES:

- VSAT NETWORKS
- DIGITAL SIGNAL PROCESSING
- DIGITAL PBX
- SECURE COMMUNICATIONS
- RADIO COMMUNICATIONS
- STUDIO SYSTEMS
- DEVELOPMENT OF TELECOMMUNICATION NETWORKS
- EDUCATION OF ELECTRONICS

One year subscription rates:

4 English issues 60 USD, 12 issues 120 USD, single issues 20 USD

Subscription orders can be sent to the publisher:

TypoTEX Ltd. H-1015 Budapest, Batthyány u. 14.
Phone: (361)202 1365; fax: (361)115 4212.

Transfer should be made to the Hungarian Foreign Trade Bank
H-1821, Budapest, Account Number 203-21411

TEKTRONIX FiberScout TFS2020
Handheld Optical Fault Finder

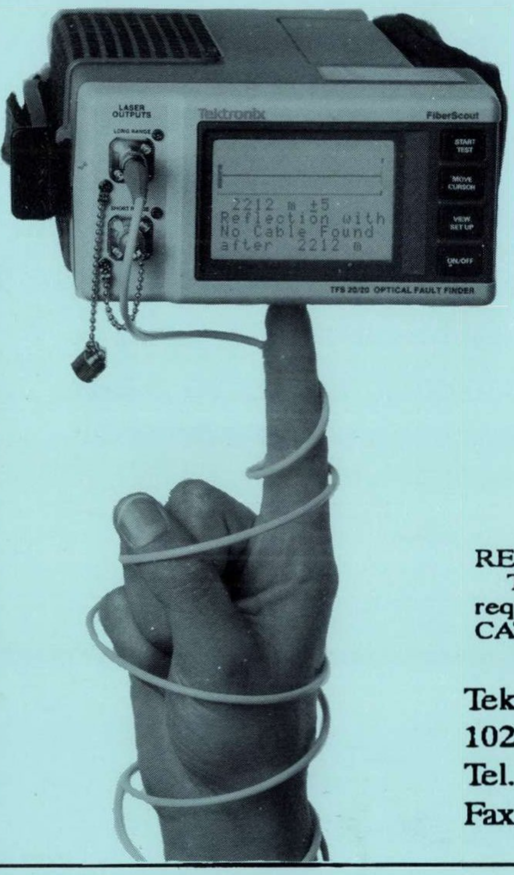

FEATURES INCLUDE:
- Simple symbolic display
  - Graphics
  - Event Description
- Fast restoration capability
- Small, lightweight, easy to handle
- 4-button operation
- Low cost – high performance
- Extended long range
- Long range
- Universal short range
- Multimode short range
- Dual port capability
- High distance accuracy
- User-selectable fault thresholds
- Internal test result storage
- RS-232C output port
  - PC
  - SEIKO DPU-201G
  - Seiko DPU-411
- PC interface software

REPRESENTATIVE USERS:
The FiberScout is designed primarily to address restoration requirements in the optical telephony, local area network and CATV environments.

Tektronix Representative
1027 Budapest, Horvát u. 2 – 12. IV.39.
Tel.: (361)201-6442
Fax: (361)156-5198

INSTALLATION
Nationwide service. Live circuit changeovers.
Turnkey project services. Make-and-lay services.
Cable recovery. Recycling of recovered materials.
Contract installation of copper/optical cables.

SYSTEMS
Major Public and Private Telecommunications networks worldwide.
Vendor-independent data, telecom, CATV and CCTV systems design, implementation and maintenance.

PROJECT MANAGEMENT
Total Quality Management:
Product, staff, project and environment.
Commitment to meeting delivery deadlines and budgets.
Customers kept informed throughout of progress.

DATACOM CABLE

Includes shielded and screened twisted copper pair. Multimode optical cable types.

TELECOM CABLE

A comprehensive range of copper, composite, and optical fibre telecommunications cables including our single-mode optical fibre cable types.
Aerial cable constructions as well as duct and buried designs, in addition to those specific to the Electricity Supply Industry.

PIRELLI CABLES LIMITED
Communication Cables Division
Wednesbury Street, Newport
Gwent NP9 OWS
United Kingdom

Hungarian Manager
H-1118 Budapest
Minerva utca 2.
Phone/Fax 361-185-2597